

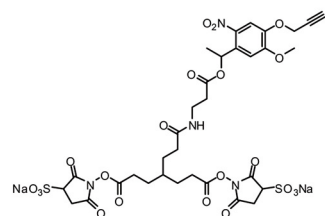


Figures and figure supplements

Trifunctional cross-linker for mapping protein-protein interaction networks and comparing protein conformational states

Dan Tan *et al*

Two-piece Leiker



sulfo-Photo-cleavable Leiker (sulfo-PL)

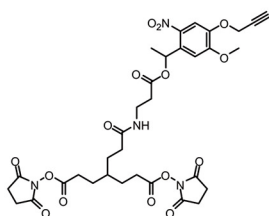
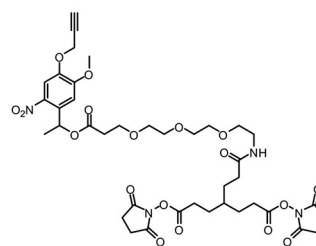
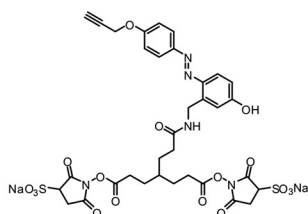


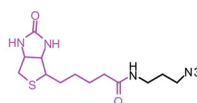
Photo-cleavable Leiker (PL)



Polyethylene glycol-Photo-cleavable Leiker (PEG-PL)

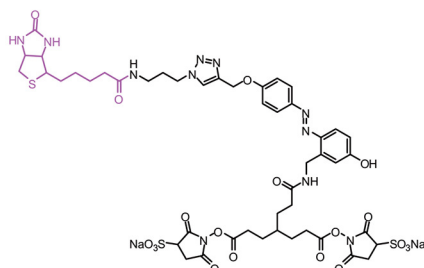


Azo-Leiker (AL)

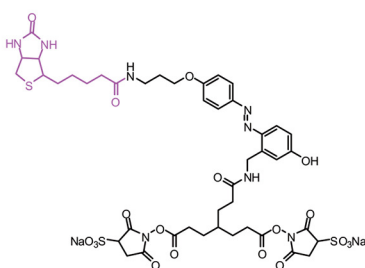


Bio-azide

One-piece Leiker



biotinylated Azo-Leiker 1 (bAL1)



biotinylated Azo-Leiker 2 (bAL2)

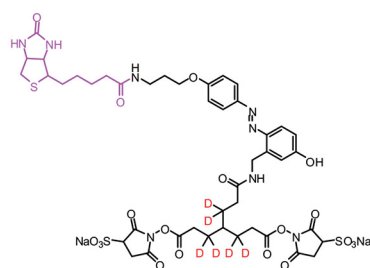
 d_6 -biotinylated Azo-Leiker 2 (d_6 -bAL2)

Figure 1. Chemical structures of different designs of Leiker. The top panel shows four designs of two-piece Leiker with a photo-cleavage site (sulfo-PL, PL, and PEG-PL) or an azobenzene-based cleavage site (AL). Biotin is attached via click chemistry by reacting with bio-azide. The bottom panel shows two unlabeled (bAL1, bAL2) and deuterium-labeled ($[d_6]$ -bAL2) one-piece Leiker molecules. The biotin moiety is colored magenta.

DOI: [10.7554/eLife.12509.003](https://doi.org/10.7554/eLife.12509.003)

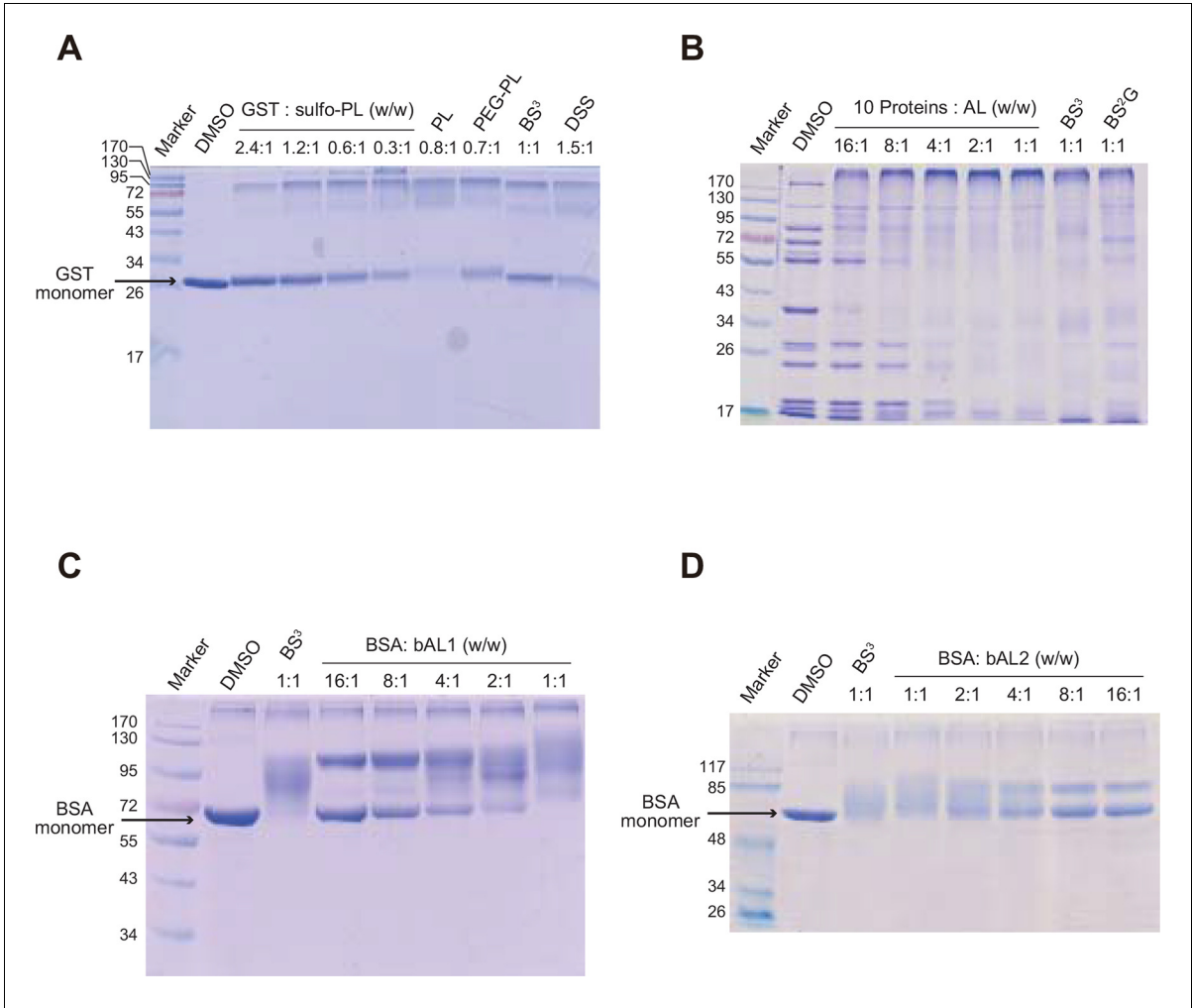


Figure 1—figure supplement 1. Optimization of protein-to-cross-linker ratio (w/w) for (A) sulfo-PL, (B) AL, (C) bAL1, and (D) bAL2.
DOI: 10.7554/eLife.12509.004

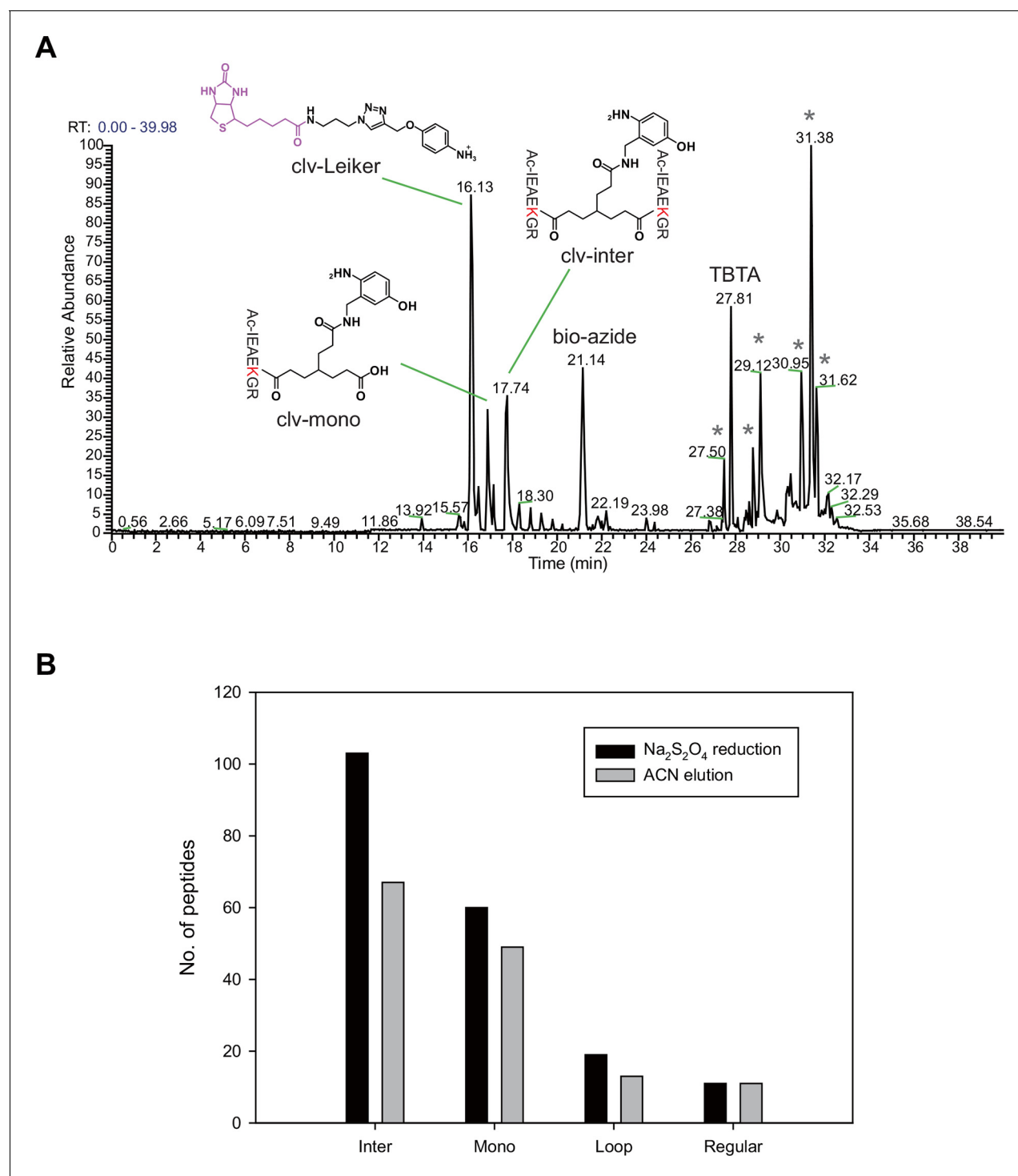


Figure 1—figure supplement 2. Evaluation of azobenzene-based chemical cleavage.

DOI: [10.7554/eLife.12509.005](https://doi.org/10.7554/eLife.12509.005)

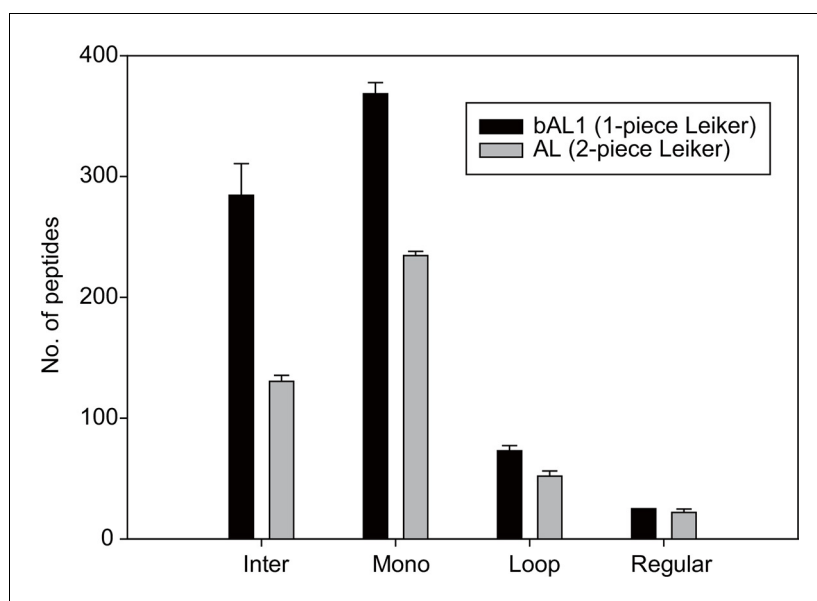


Figure 1—figure supplement 3. The one-piece Leiker (bAL1) outperformed the two-piece Leiker (AL) in the CXMS analysis of a mixture of ten standard proteins.

DOI: [10.7554/eLife.12509.006](https://doi.org/10.7554/eLife.12509.006)

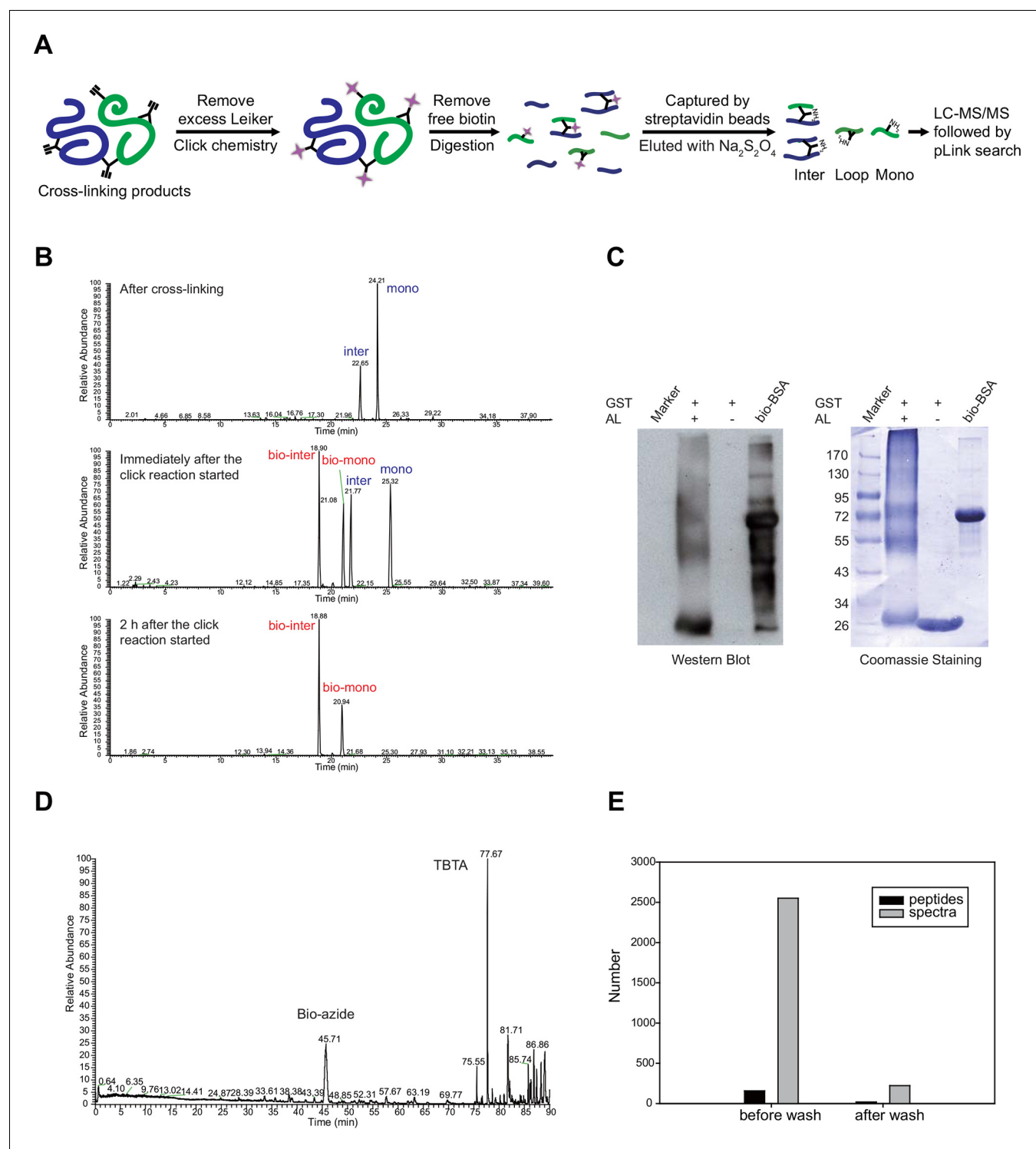


Figure 1—figure supplement 4. Evaluation of the two piece Azo-Leiker (AL).

DOI: [10.7554/eLife.12509.007](https://doi.org/10.7554/eLife.12509.007)

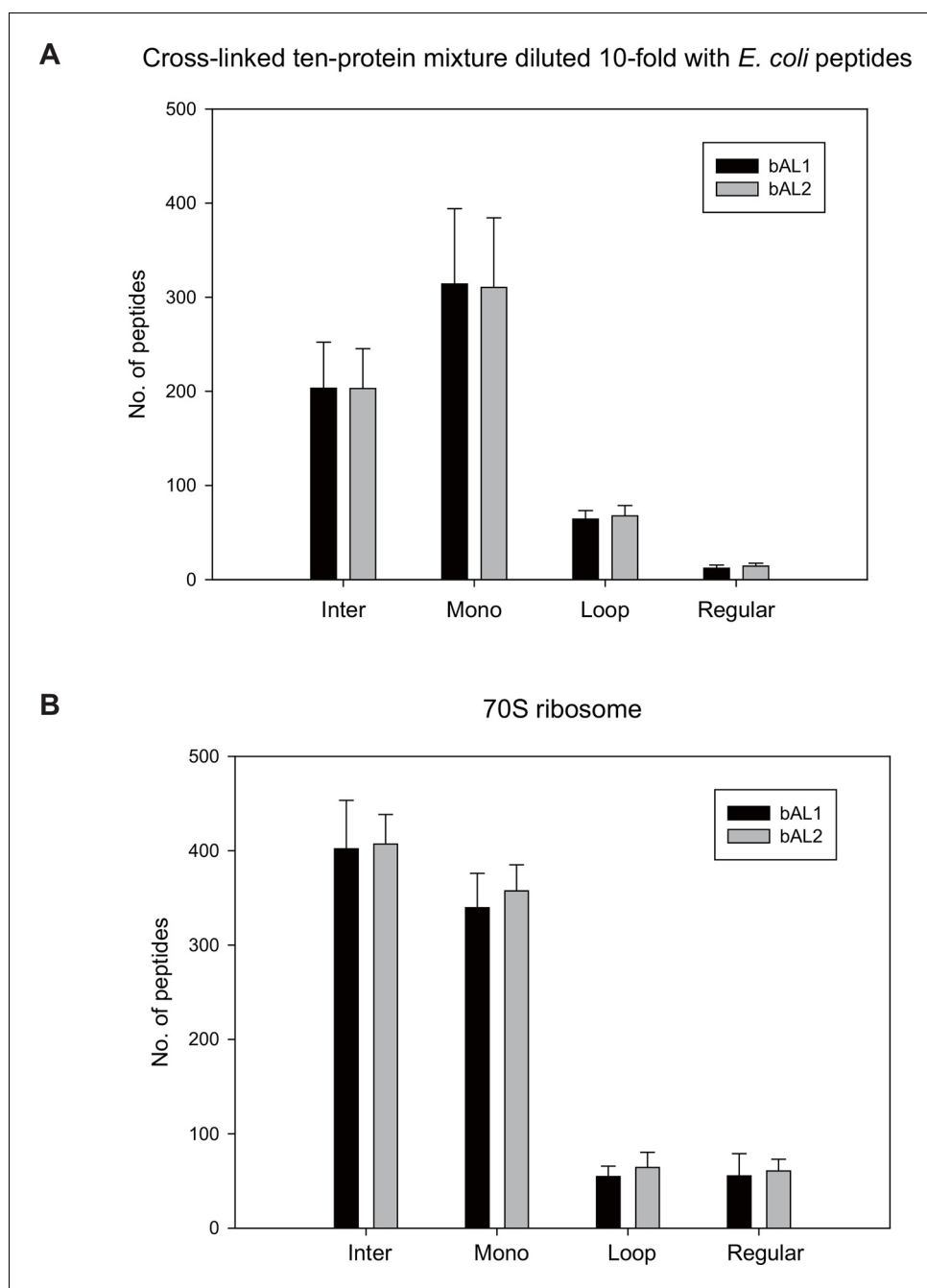


Figure 1—figure supplement 5. bAL1 and bAL2 performed similarly.

[DOI: 10.7554/eLife.12509.008](https://doi.org/10.7554/eLife.12509.008)

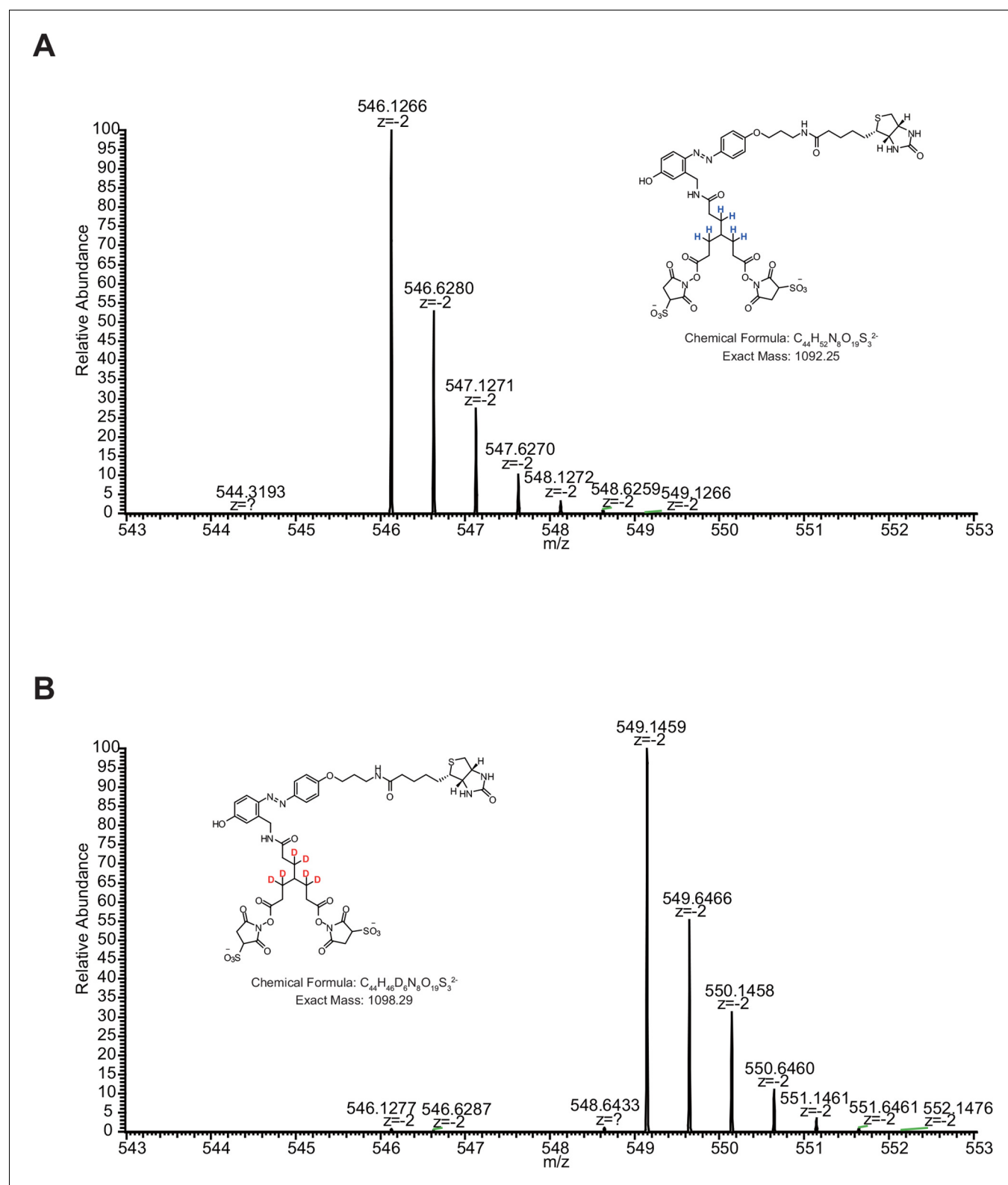


Figure 1—figure supplement 6. MS1 spectra of (A) $[d_0]$ -bAL2 and (B) $[d_6]$ -bAL2.

DOI: [10.7554/eLife.12509.009](https://doi.org/10.7554/eLife.12509.009)

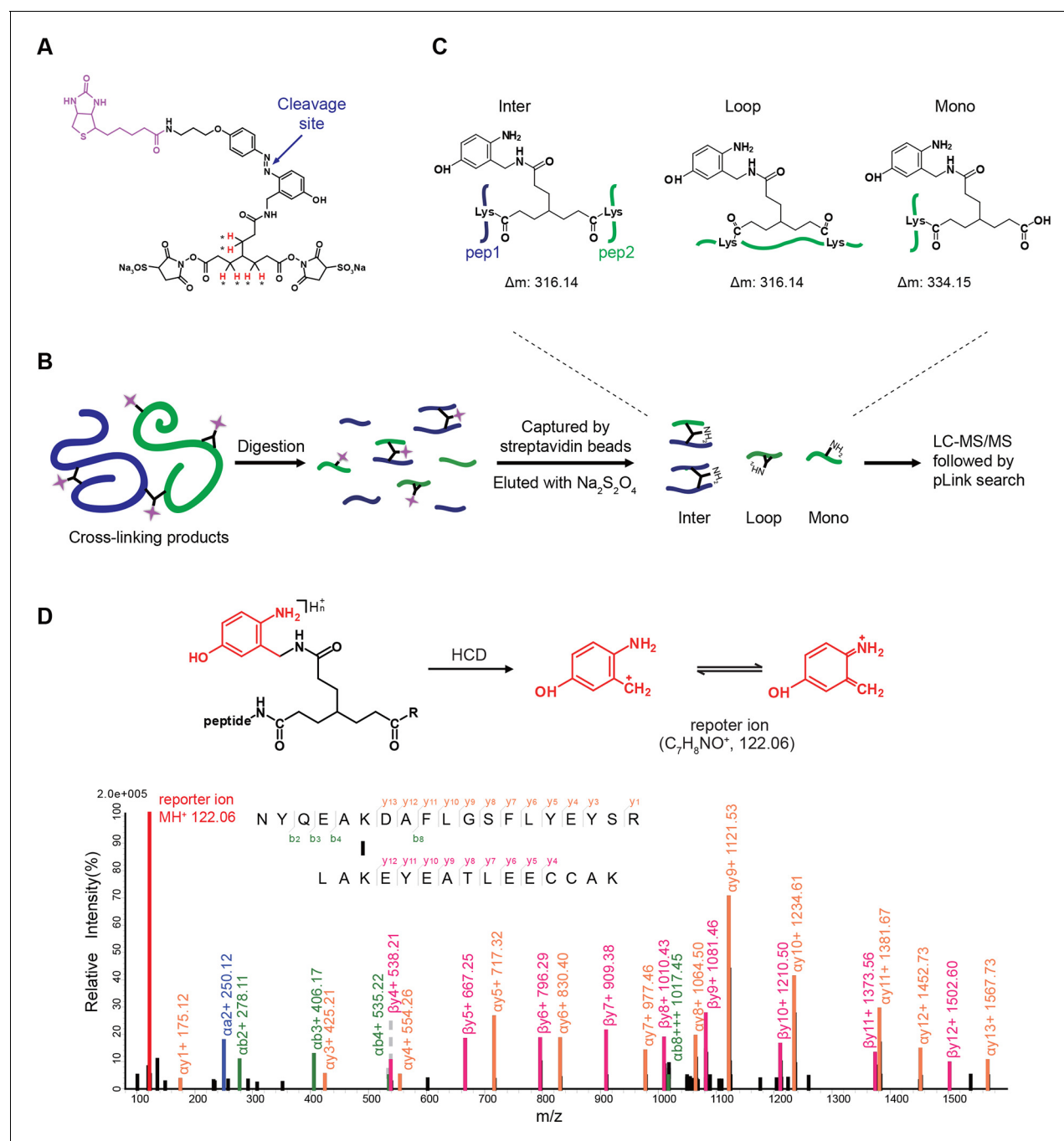


Figure 2. Scheme of the Leiker-based CXMS workflow. (A) Leiker contains a biotin moiety (magenta), a cleavage site (arrows), and six hydrogen atoms that are accessible to isotope labeling (asterisks). (B) The workflow for purification of Leiker-linked peptides. (C) Three types of Leiker-linked peptides. (D) Leiker-linked peptides generate a reporter ion of 122.06 m/z in HCD, as shown in the spectrum of an inter-linked peptide NYQEAKDAFLGSLFLEYEYSR-LAKEYEATLEECCA ($+4$ charged, MH^+ 4433.0553), in which C denotes carbamidomethylated cysteine.

DOI: 10.7554/eLife.12509.010

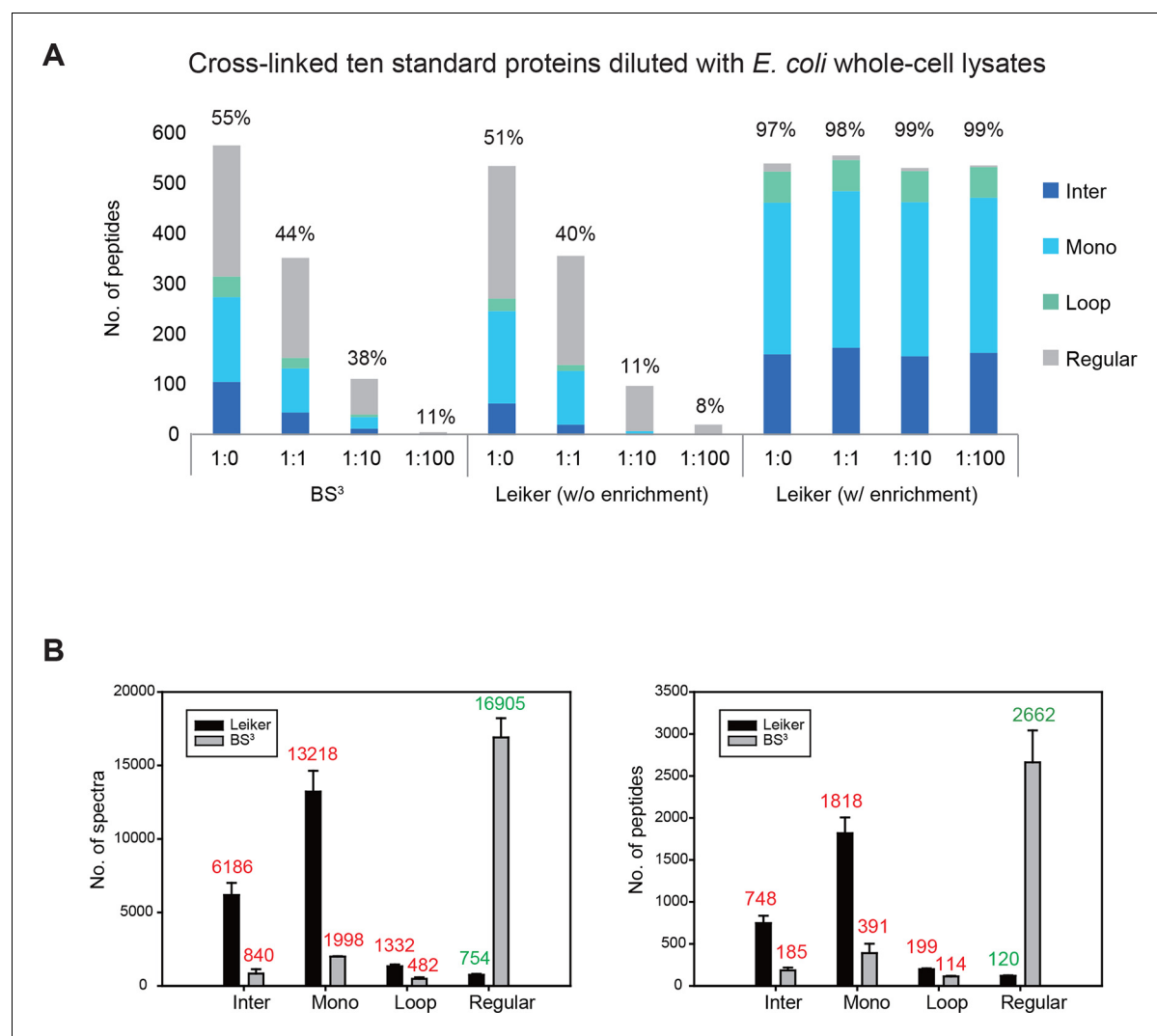


Figure 3. Evaluating the performance of Leiker. (A) Leiker allowed near 100% enrichment of target peptides from a cross-linked ten-protein mixture diluted with increasing amounts of non-cross-linked *E. coli* lysates. Dark blue, inter-links; light blue, mono-links; green, loop-links; grey, regular peptides not modified by Leiker. (B) Number of cross-link identifications from *E. coli* lysates treated with Leiker or BS³. Shown in the left and right panels are the identified spectra and peptides, respectively.

DOI: [10.7554/eLife.12509.011](https://doi.org/10.7554/eLife.12509.011)

The following source data is available for figure 3:

Source data 1. Ten standard proteins used to evaluate Leiker, mixed at equal amounts by mass.

DOI: [10.7554/eLife.12509.012](https://doi.org/10.7554/eLife.12509.012)

Source data 2. Summary of identified spectra from the ten-protein mixture.

DOI: [10.7554/eLife.12509.013](https://doi.org/10.7554/eLife.12509.013)

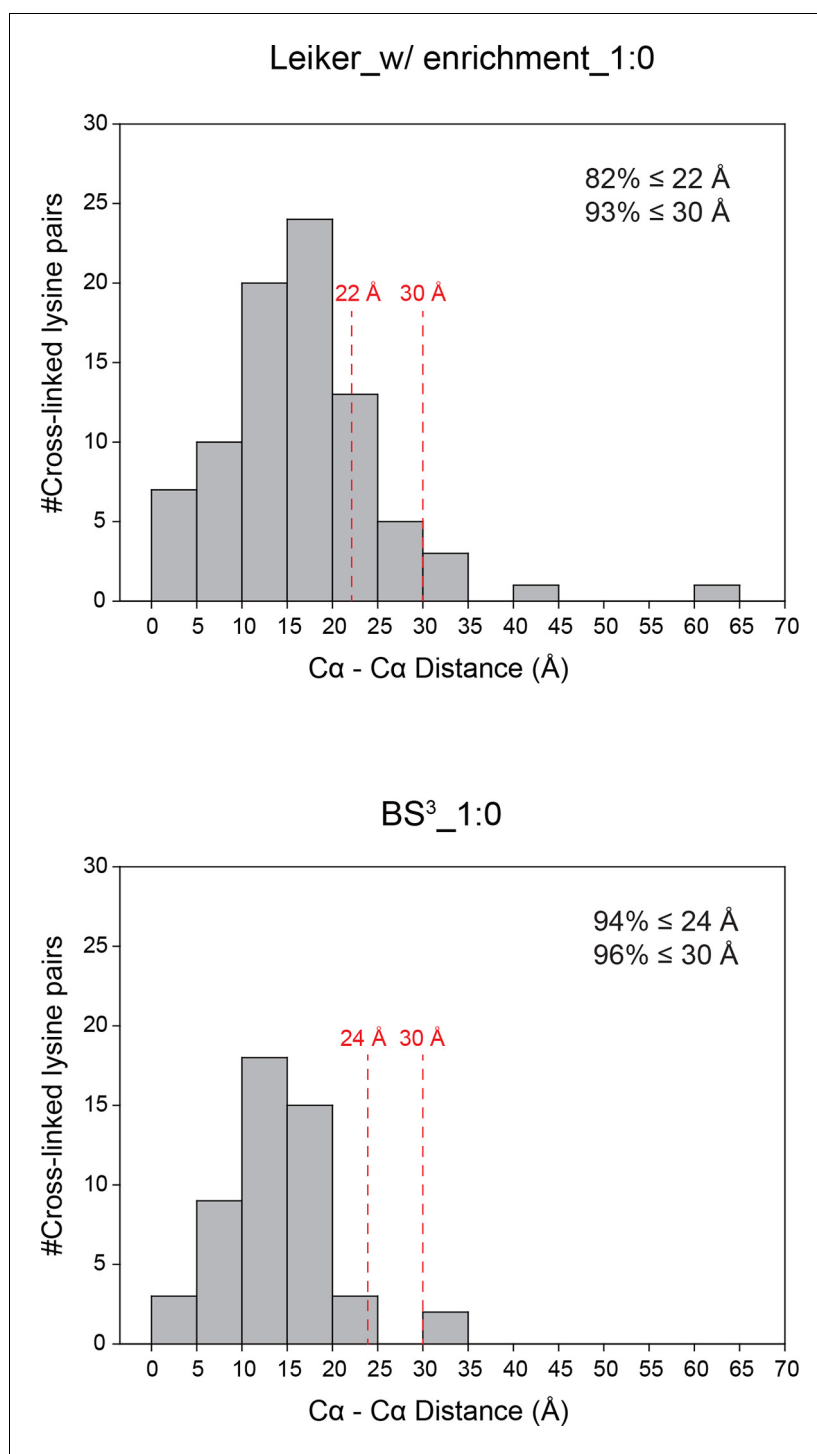


Figure 3—figure supplement 1. Distance distributions of cross-linked lysine pairs in the undiluted ten-protein mixture.

DOI: [10.7554/eLife.12509.014](https://doi.org/10.7554/eLife.12509.014)

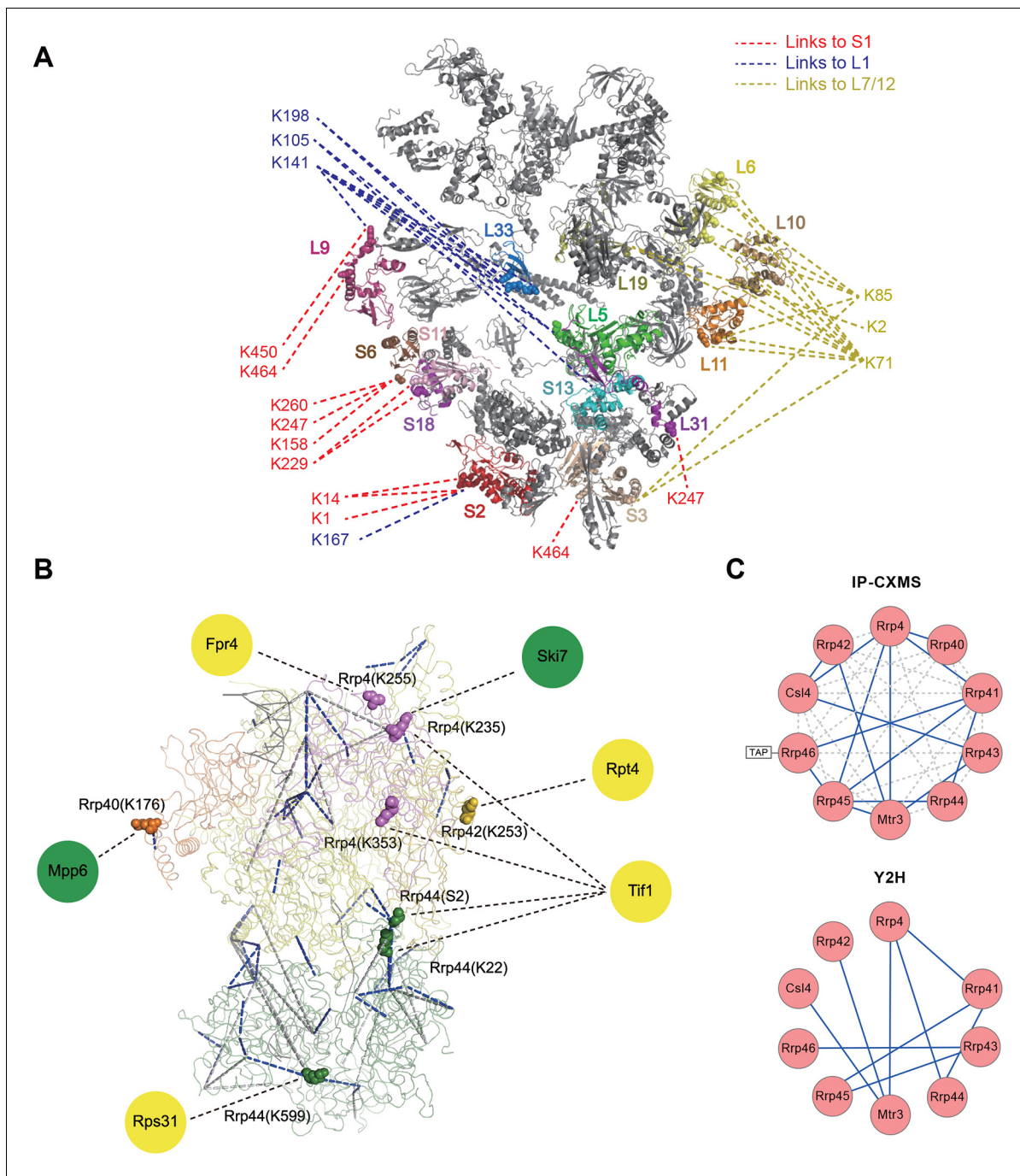


Figure 4. Leiker-based CXMS analyses of large protein assemblies. **(A)** Analysis of a purified *E. coli* 70S ribosome revealed the locations of highly dynamic periphery ribosomal proteins S1, L1, and L7/12 that were refractory to crystallography and cryo-EM analysis. Cross-links to S1, L1, and L7/12 are colored red, blue, and yellow, respectively, and the cross-linked residues on these three proteins are numbered according to the Uniprot sequences. **(B)** Analysis of a crude immunoprecipitate of the yeast exosome complex. Dashed blue and grey lines denote 50 compatible and 22 incompatible cross-links, respectively, according to the structure of the RNA-bound 11-subunit exosome complex (PDB code: 4IFD). Rrp44, green; Rrp40, orange; Rrp4, violet; Rrp42, gold; other exosome subunits, yellow; RNA, black. Known and candidate exosome regulators revealed by Leiker-cross-links are shown along the periphery and highlighted in green and yellow circles, respectively. **(C)** Connectivity maps of the ten-subunit exosome core complex based on the inter-molecular cross-links identified in the current IP-CXMS experiments or on previous yeast two-hybrid (Y2H) studies (Stark et al., 2006; Uetz et al., 2000; Oliveira et al., 2002; Luz et al., 2007; Yu et al., 2008). Blue solid lines: experimentally identified putative direct protein-protein interactions; grey dashed lines: theoretical cross-links according to the crystal structure; C α -C α distance cutoff ≤ 30 Å.

DOI: 10.7554/eLife.12509.015

Figure 4 continued on next page

Figure 4 continued

The following source data is available for figure 4:

Source data 1. CXMS analysis of *E. coli* 70S ribosomes.

DOI: [10.7554/eLife.12509.016](https://doi.org/10.7554/eLife.12509.016)

Source data 2. Number of cross-linked lysine pairs classified by ribosomal proteins.

DOI: [10.7554/eLife.12509.017](https://doi.org/10.7554/eLife.12509.017)

Source data 3. Identified cross-linked lysine pairs involving L1.

DOI: [10.7554/eLife.12509.018](https://doi.org/10.7554/eLife.12509.018)

Source data 4. CXMS analysis of the *Saccharomyces cerevisiae* exosome complex.

DOI: [10.7554/eLife.12509.019](https://doi.org/10.7554/eLife.12509.019)

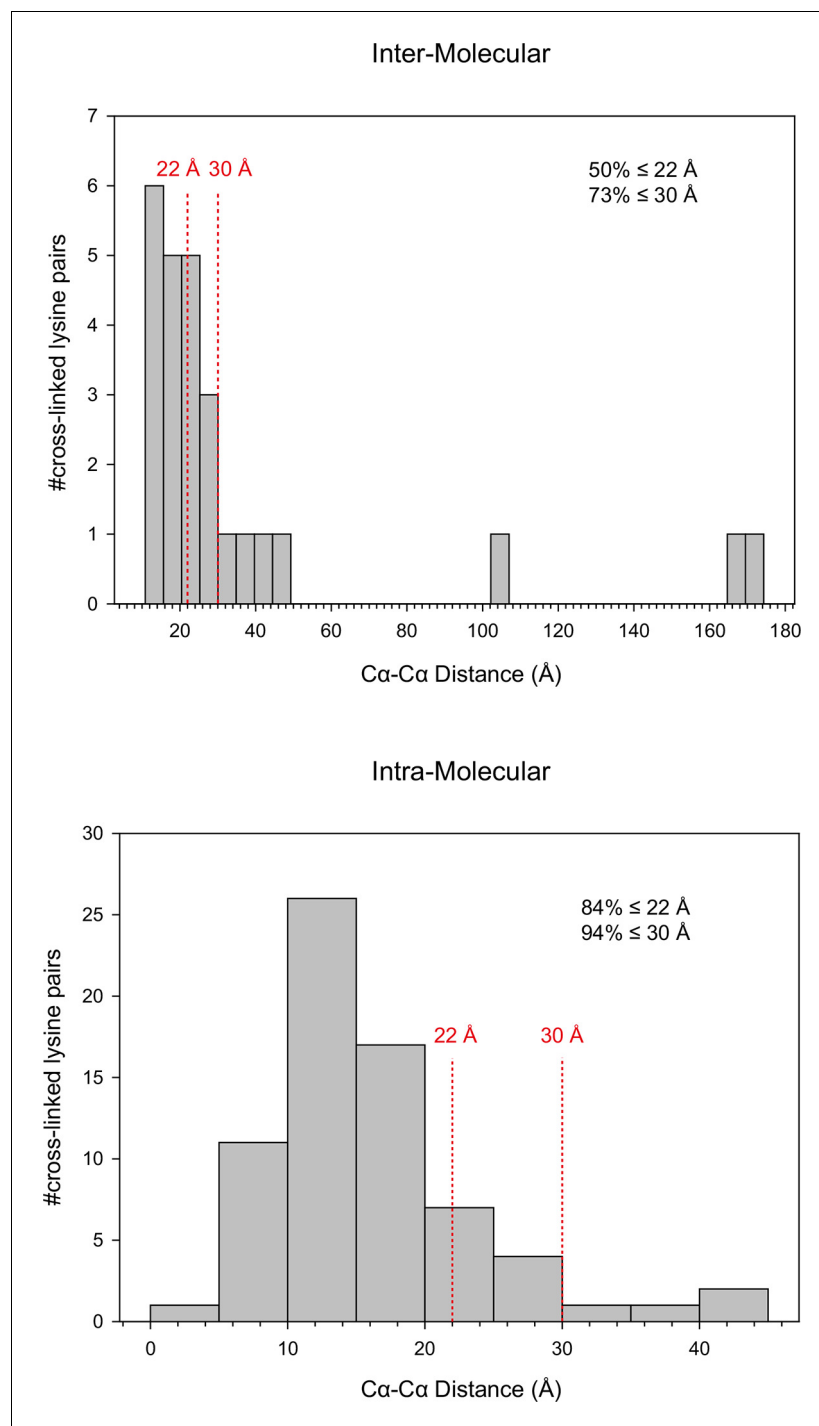


Figure 4—figure supplement 1. Distance distribution of the inter-molecular and intra-molecular cross-links identified in 70S ribosomes.

DOI: [10.7554/eLife.12509.020](https://doi.org/10.7554/eLife.12509.020)

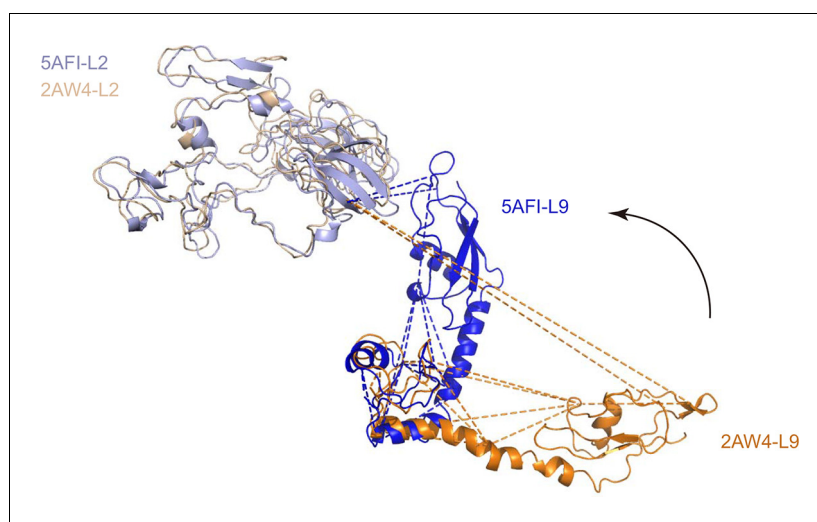


Figure 4—figure supplement 2. Alignment of L9 and L2 from the crystal structure (L9, orange; L2, wheat; PDB code: 2AW4) and their counterparts from the cryo-EM reconstruction (L9, blue; L2, lightblue; PDB code: 5AFI).
DOI: [10.7554/eLife.12509.021](https://doi.org/10.7554/eLife.12509.021)

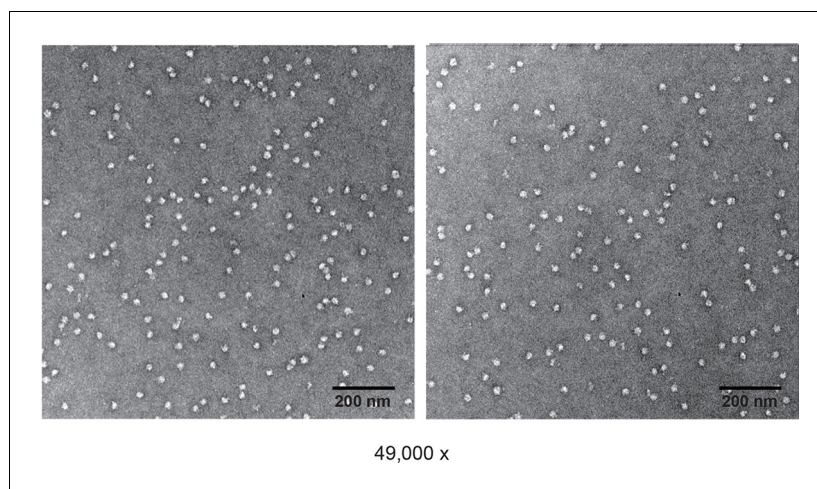


Figure 4—figure supplement 3. Negative staining of non-cross-linked *E. coli* 70S ribosome.
[DOI: 10.7554/eLife.12509.022](https://doi.org/10.7554/eLife.12509.022)

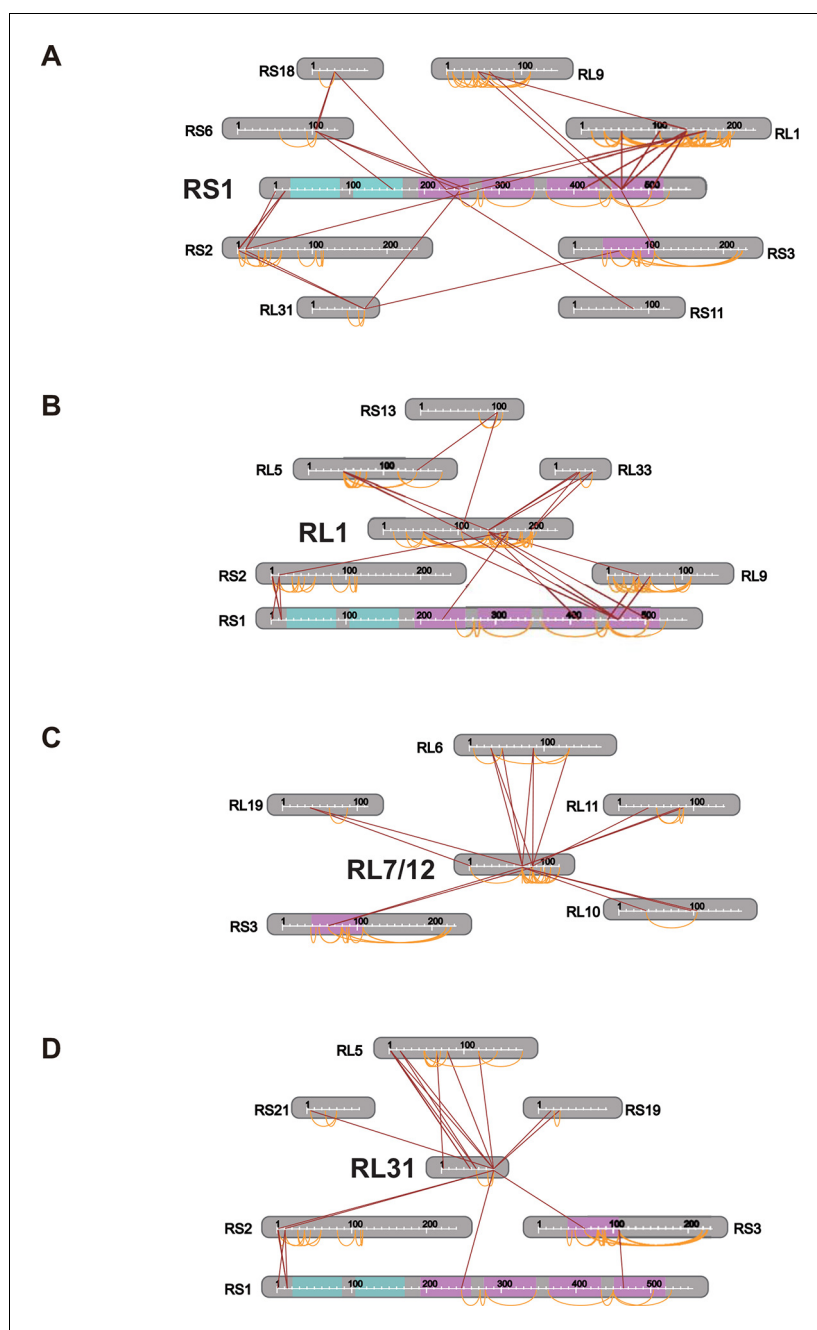


Figure 4—figure supplement 4. Connectivity maps of cross-links involving (A) S1, (B) L1, (C) L7/12, and (D) L31.
DOI: [10.7554/eLife.12509.023](https://doi.org/10.7554/eLife.12509.023)

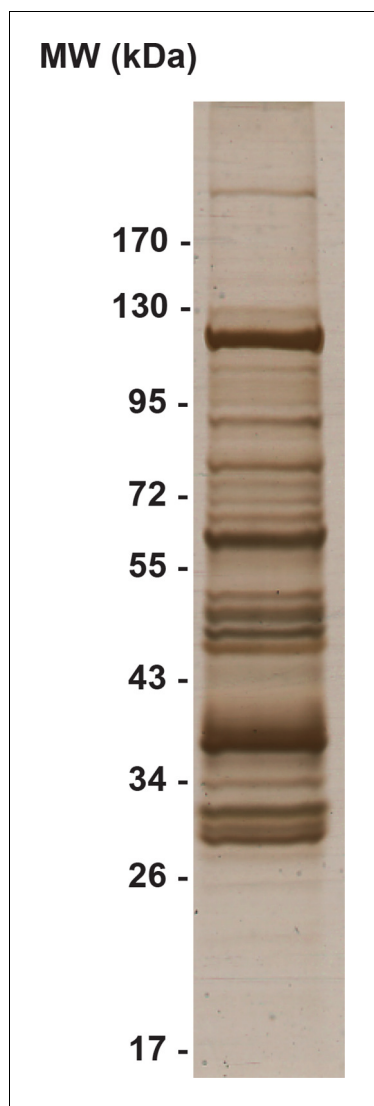


Figure 4—figure supplement 5. Silver-stained SDS-PAGE gel of the crude immunoprecipitate of TAP-tagged Rrp46.
DOI: [10.7554/eLife.12509.024](https://doi.org/10.7554/eLife.12509.024)

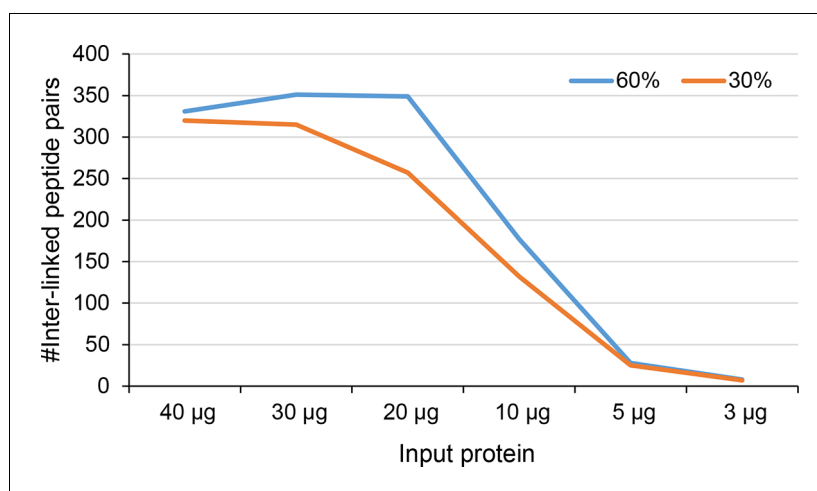


Figure 4—figure supplement 6. Number of identified inter-linked peptide pairs from decreasing amount of Leiker-cross-linked exosome immunoprecipitate (FDR < 0.05, E-value < 0.01). After enrichment, 30% (orange) or 60% (blue) of each sample was analyzed by LC-MS/MS.

DOI: [10.7554/eLife.12509.025](https://doi.org/10.7554/eLife.12509.025)

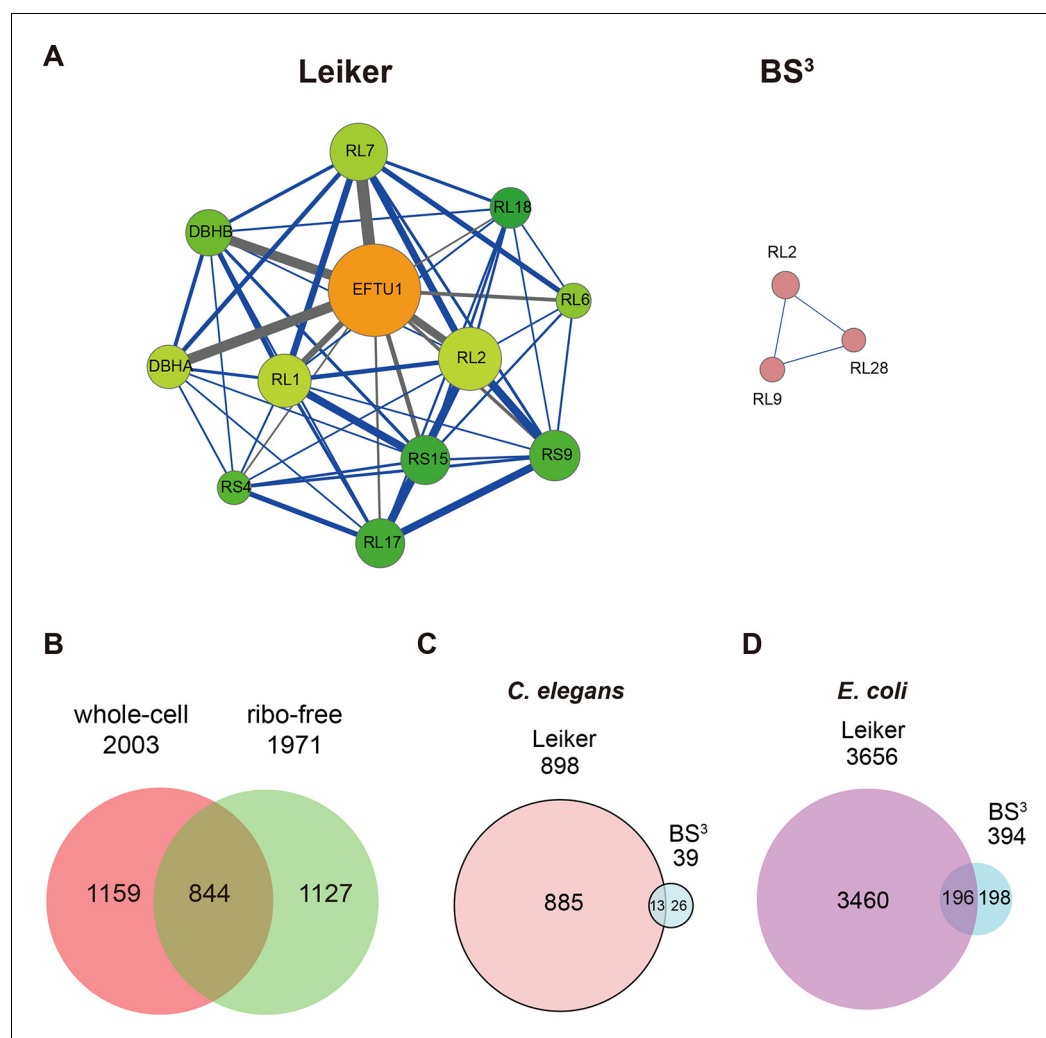


Figure 5. CXMS analyses of *E. coli* and *C. elegans* lysates. (A) The best protein-protein interaction cluster extracted from the Leiker-identified or BS³-identified (Yang et al., 2012) inter-links from *E. coli* whole-cell lysates. Node size represents the degree of connectivity of the indicated protein in the network. Line width represents the spectral counts of every inter-molecular cross-link. The line color is set to blue when the two peptides of an inter-link are both attributed to unique proteins, to grey if either could be assigned to multiple proteins. All the lines connected to EF-Tu1 are grey because EF-Tu1 differs from EF-Tu2 by only one amino acid. (B) Comparison of the identified inter-links in *E. coli* whole-cell lysates and ribo-free lysates (5% FDR, E-value < 0.01, spectral count ≥ 3). (C and D) Comparison of the number of Leiker-identified inter-links and that of BS³-identified inter-links (Yang et al., 2012) from *C. elegans* (C) and *E. coli* (D) whole-cell lysates (5% FDR, E-value < 0.01, spectral count ≥ 1).

DOI: 10.7554/eLife.12509.026

The following source data is available for figure 5:

Source data 1. CXMS analysis of *E. coli* whole-cell lysates.

DOI: 10.7554/eLife.12509.027

Source data 2. CXMS analysis of *E. coli* ribo-free lysates.

DOI: 10.7554/eLife.12509.028

Source data 3. CXMS analysis of *C. elegans* whole-cell lysates.

DOI: 10.7554/eLife.12509.029

Source data 4. CXMS analysis of *C. elegans* mitochondrial proteins.

DOI: 10.7554/eLife.12509.030

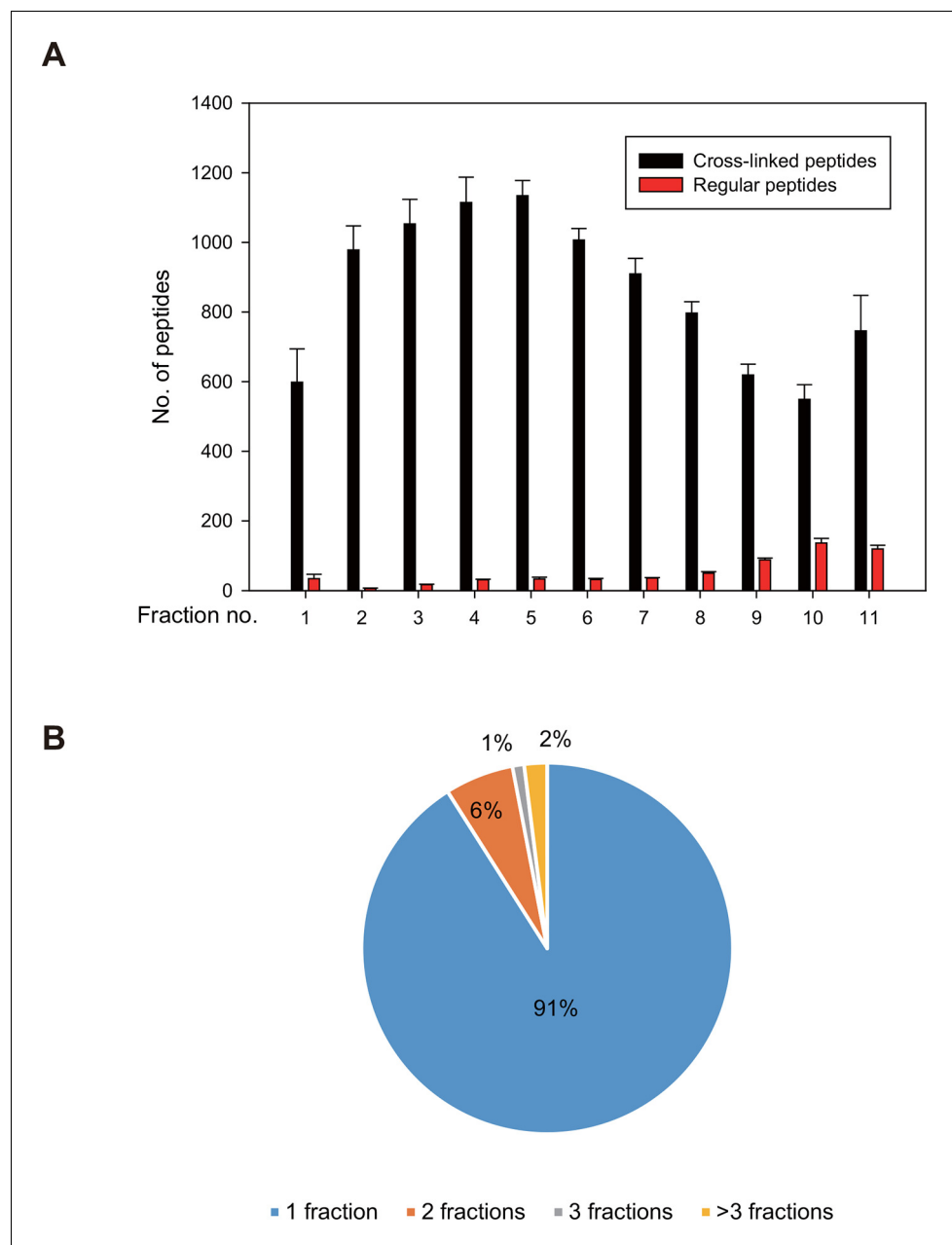


Figure 5—figure supplement 1. Fractionation of digested, Leiker-treated *E. coli* lysates.

DOI: [10.7554/eLife.12509.031](https://doi.org/10.7554/eLife.12509.031)

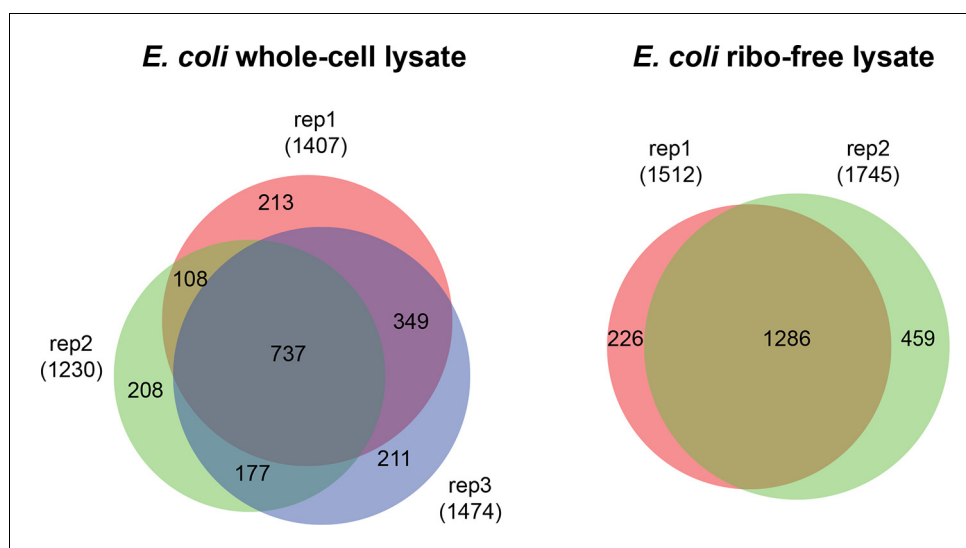
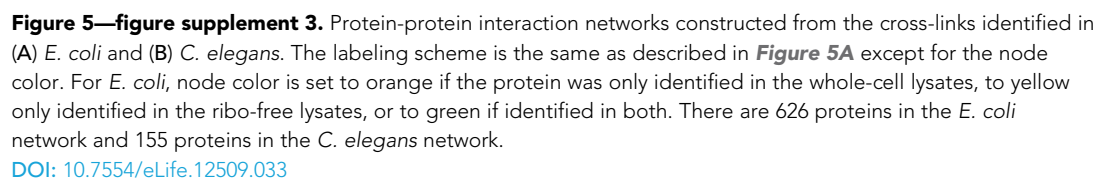


Figure 5—figure supplement 2. Overlap of cross-linked lysine pairs between biological replicates of *E. coli* lysates (FDR < 0.05, E-value < 0.01, and spectral count ≥ 3).

DOI: [10.7554/eLife.12509.032](https://doi.org/10.7554/eLife.12509.032)



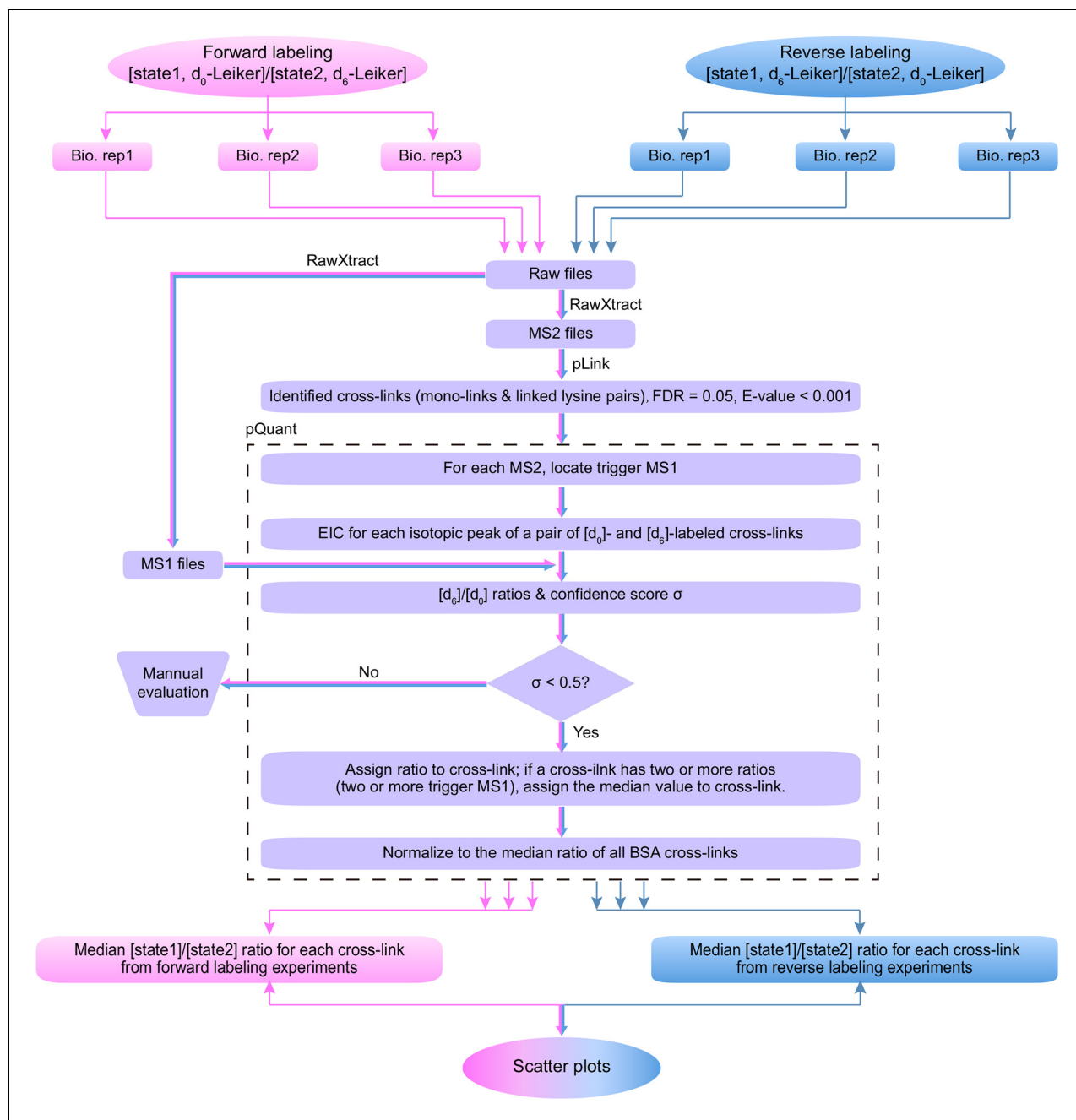


Figure 6. Workflow for quantification of cross-linked peptides using pQuant. For each identified cross-link spectrum, an extracted ion chromatogram (EIC) is constructed for each isotopic peak of the $[d_0]$ - and $[d_6]$ -labeled precursor. The $[d_6]/[d_0]$ ratios can be calculated based on the monoisotopic peak, the most intense peak, or the least interfered peak of each isotopic cluster as specified by users. The accuracy of the ratio calculation was evaluated with the confidence score σ (range: 0–1, from the most to the least reliable). If a cross-link have ratios with $\sigma < 0.5$, the median of these ratios is assigned to this cross-link. The cross-link ratios of the proteins of interest are normalized to the median ratio of all BSA cross-links. For each cross-link, the median $[state1]/[state2]$ ratio of three independent forward labeling experiments is plotted against the median ratio of three independent reverse labeling experiments. Cross-links that are only present in state1 or state2 due to a dramatic conformational change cannot be quantified as described above because the ratios would be zero or infinite and their σ values would be 1. Therefore, if a cross-link does not have a valid ratio after automatic quantification, the EICs were manually inspected to determine if it was an all-or-none change.

DOI: [10.7554/eLife.12509.034](https://doi.org/10.7554/eLife.12509.034)

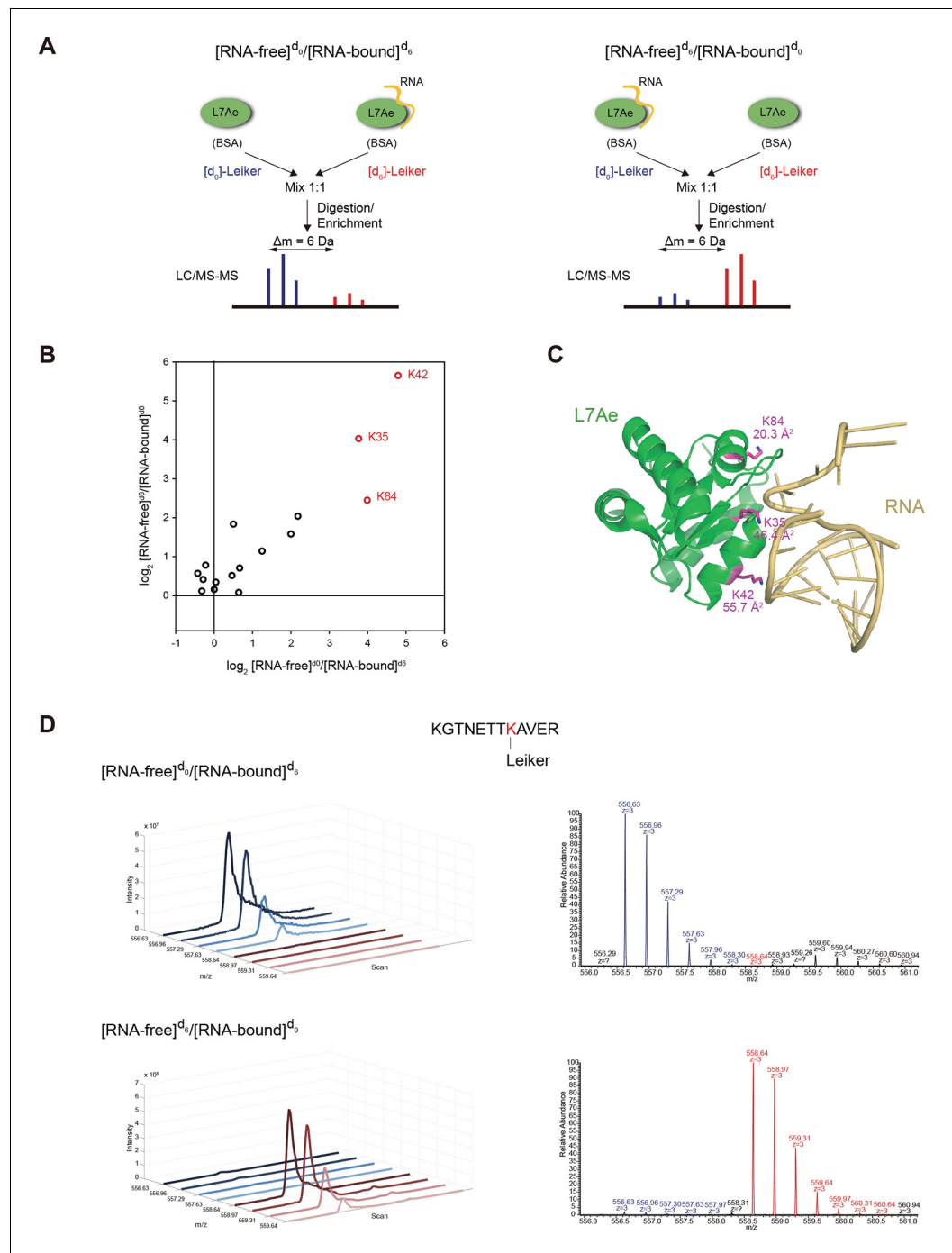


Figure 7. Quantitative CXMS analysis of the L7Ae-RNA complex. (A) Reciprocal labeling of RNA-free (F) and RNA-bound (B) L7Ae with $[d_0]/[d_6]$ -Leiker. (B) Abundance ratios of mono-links (F/B) in the forward ($F^{[d_0]}/B^{[d_6]}$) and the reverse labeling experiment ($F^{[d_6]}/B^{[d_0]}$). Each circle represents a mono-linked lysine residue and is colored red if it has a ratio greater than five in both labeling schemes. (C) The three lysine residues affected by RNA binding are highlighted in the structure model (PDB code: 2HVY). The number below each such lysine residue indicates the buried surface area (\AA^2) upon RNA binding. (D) Extracted ion chromatograms (left) and representative MS1 spectra (right) of a K42 mono-link.

DOI: 10.7554/eLife.12509.035

The following source data is available for figure 7:

Source data 1. Quantitative CXMS analysis of L7Ae with or without the H/ACA RNA.

DOI: 10.7554/eLife.12509.036

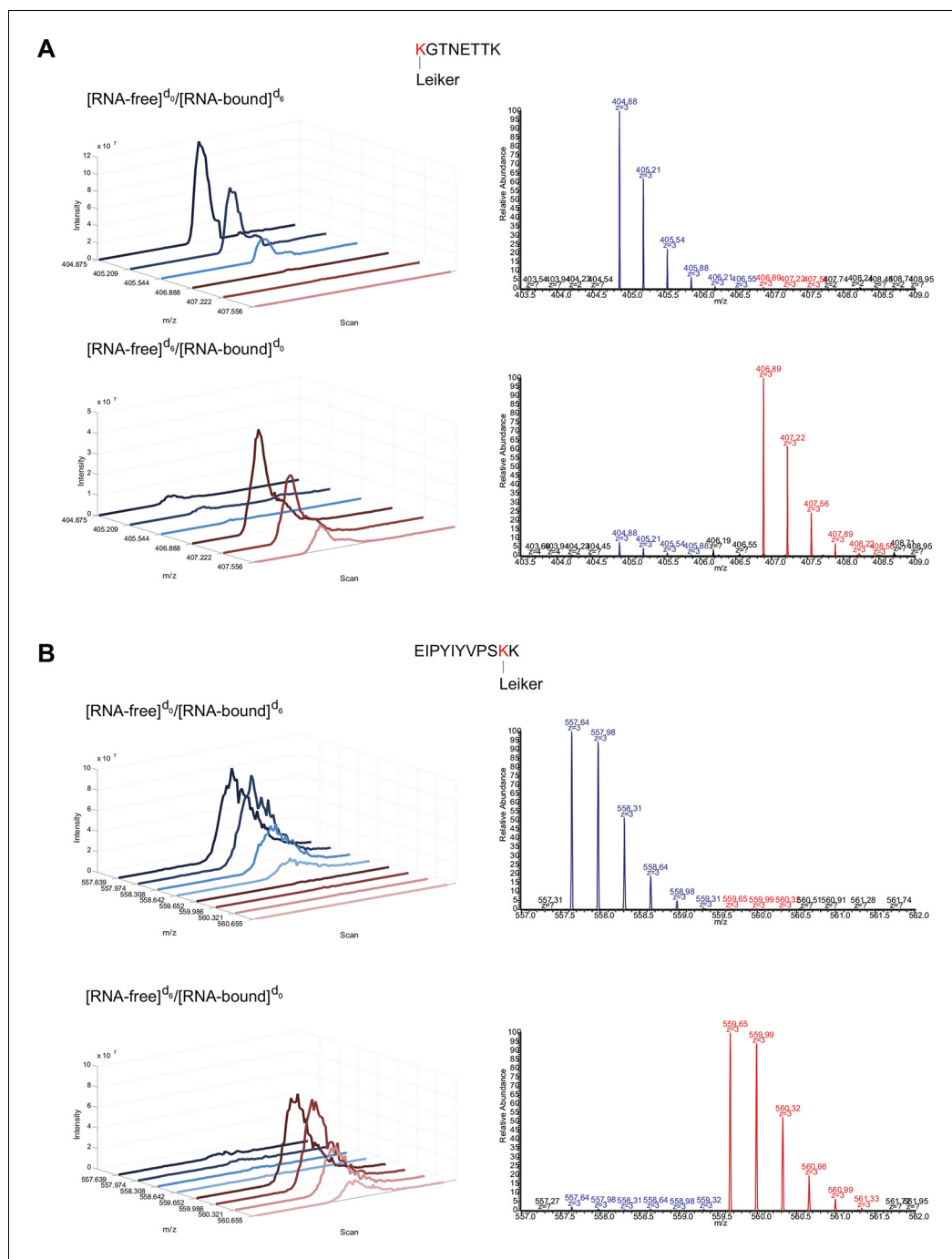


Figure 7—figure supplement 1. Extracted ion chromatograms (left) and representative MS1 spectra (right) of a mono-linked peptide corresponding to (A) K35 and (B) K84.

DOI: [10.7554/eLife.12509.037](https://doi.org/10.7554/eLife.12509.037)

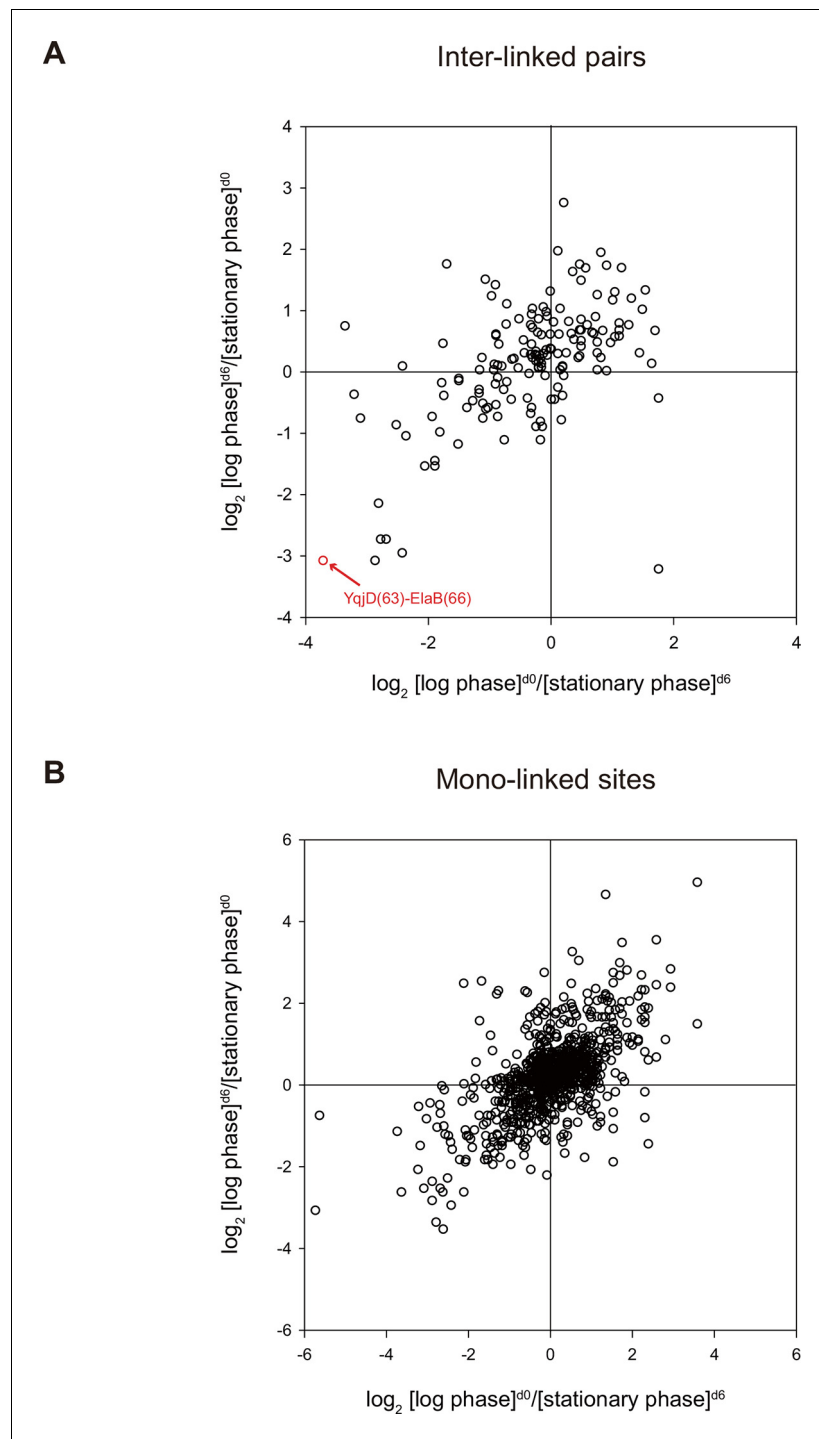


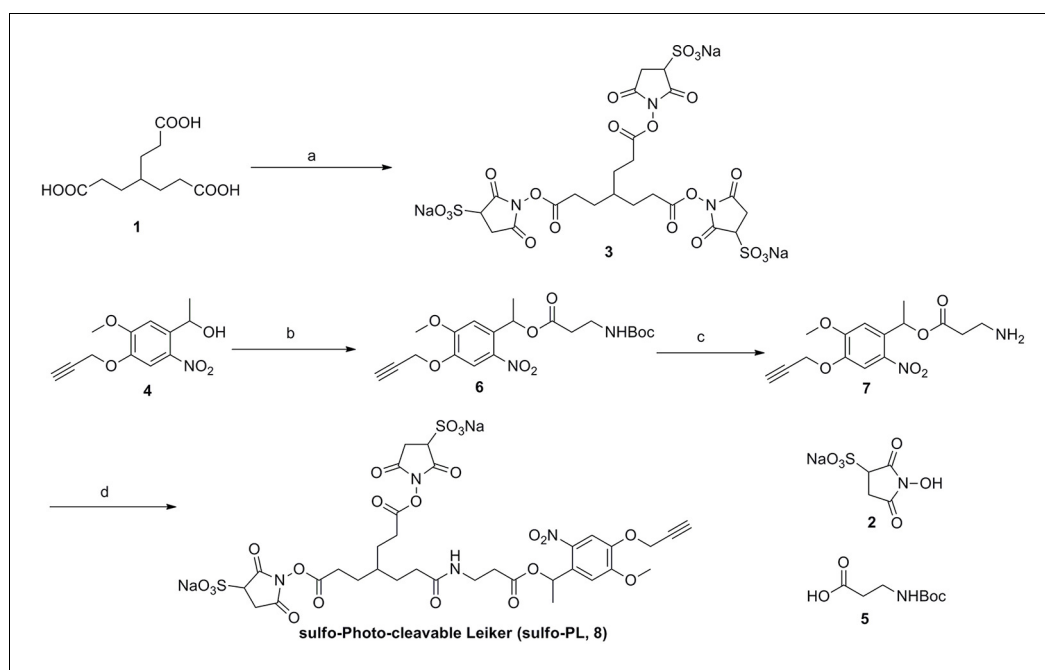
Figure 8. Quantitative CXMS analysis of *E. coli* lysates. Abundance ratios of (A) inter-linked lysine pairs and (B) mono-linked sites in the forward ($[\log \text{phase}]^{d0} / [\text{stationary phase}]^{d6}$) and the reverse labeling experiment ($[\log \text{phase}]^{d6} / [\text{stationary phase}]^{d0}$).

DOI: [10.7554/eLife.12509.038](https://doi.org/10.7554/eLife.12509.038)

The following source data is available for figure 8:

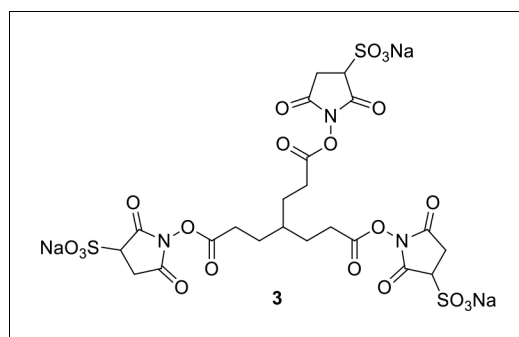
Source data 1. Quantitative CXMS analysis of *E. coli* lysates.

DOI: [10.7554/eLife.12509.039](https://doi.org/10.7554/eLife.12509.039)



Appendix 1—figure 1. Synthesis of sulfo-Photo-cleavable Leiker (sulfo-PL, 8)

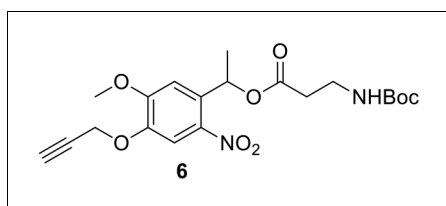
DOI: [10.7554/eLife.12509.040](https://doi.org/10.7554/eLife.12509.040)



Appendix 1—figure 2.

Compound 3.

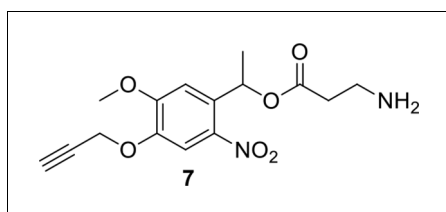
[DOI: 10.7554/eLife.12509.041](https://doi.org/10.7554/eLife.12509.041)



Appendix 1—figure 3.

Compound 6.

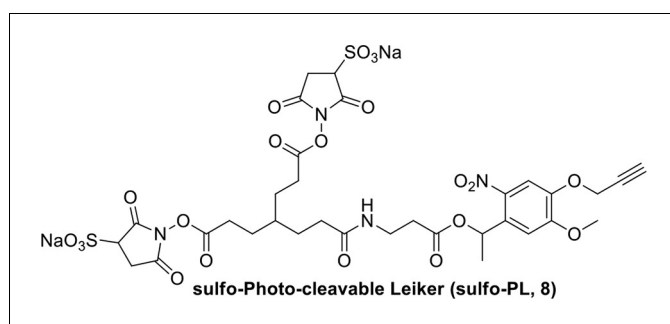
DOI: [10.7554/eLife.12509.042](https://doi.org/10.7554/eLife.12509.042)



Appendix 1—figure 4.

Compound 7.

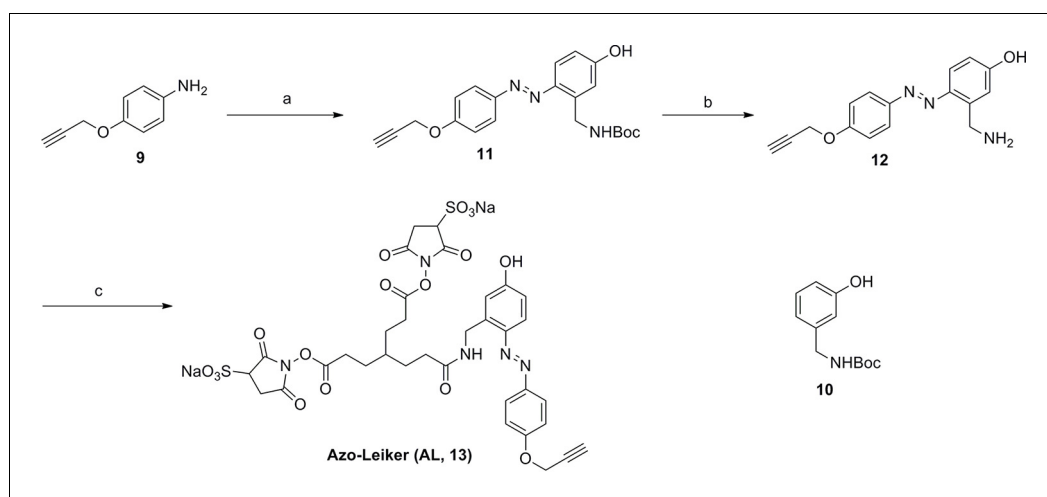
DOI: [10.7554/eLife.12509.043](https://doi.org/10.7554/eLife.12509.043)



Appendix 1—figure 5.

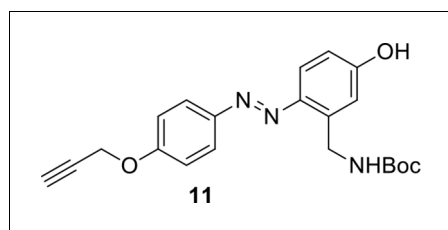
Compound 8.

DOI: [10.7554/eLife.12509.044](https://doi.org/10.7554/eLife.12509.044)

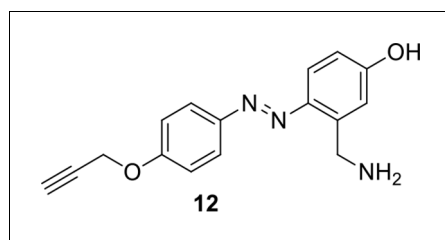


Appendix 1—figure 6. Synthesis of Azo-Leiker (AL, 13).

DOI: [10.7554/eLife.12509.045](https://doi.org/10.7554/eLife.12509.045)

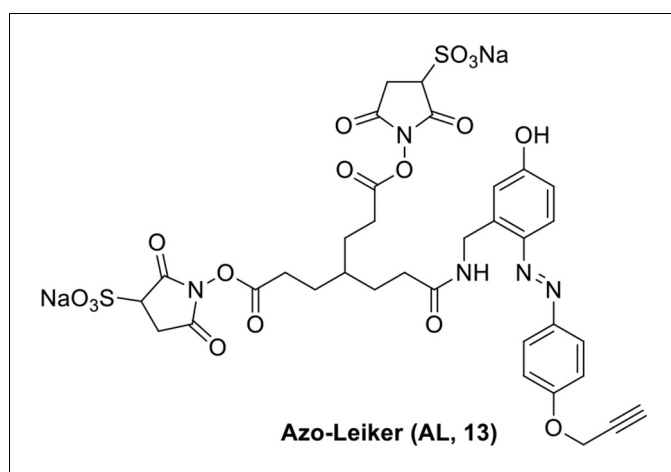


Appendix 1—figure 7. Compound 11.
DOI: [10.7554/eLife.12509.046](https://doi.org/10.7554/eLife.12509.046)



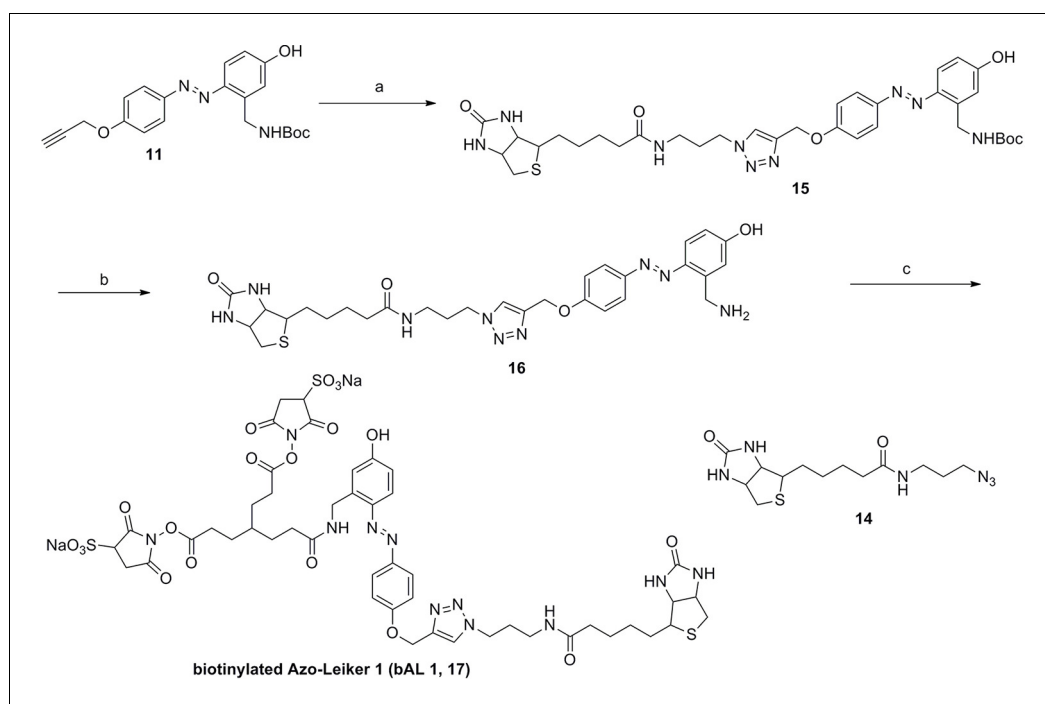
Appendix 1—figure 8. Compound 12.

DOI: [10.7554/eLife.12509.047](https://doi.org/10.7554/eLife.12509.047)



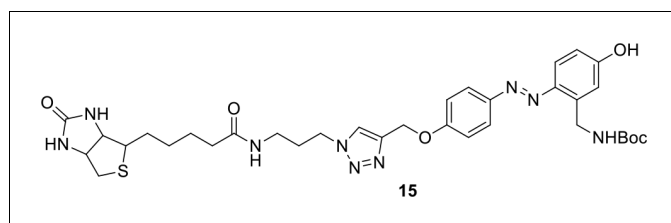
Appendix 1—figure 9. Compound 13.

DOI: [10.7554/eLife.12509.048](https://doi.org/10.7554/eLife.12509.048)



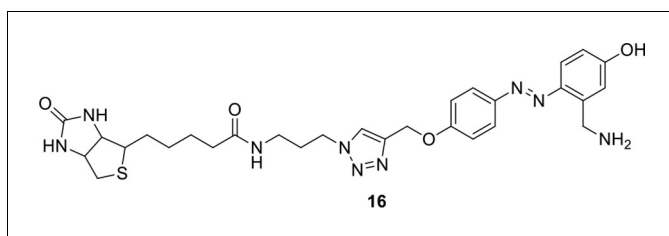
Appendix 1—figure 10. Synthesis of biotinylated Azo-Leiker 1 (bAL 1, 17).

DOI: [10.7554/eLife.12509.049](https://doi.org/10.7554/eLife.12509.049)



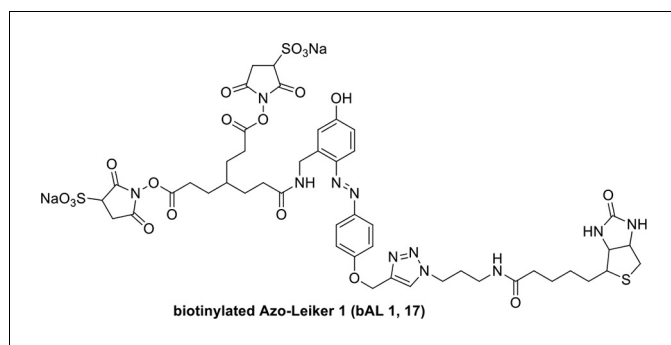
Appendix 1—figure 11. Compound 15.

DOI: [10.7554/eLife.12509.050](https://doi.org/10.7554/eLife.12509.050)



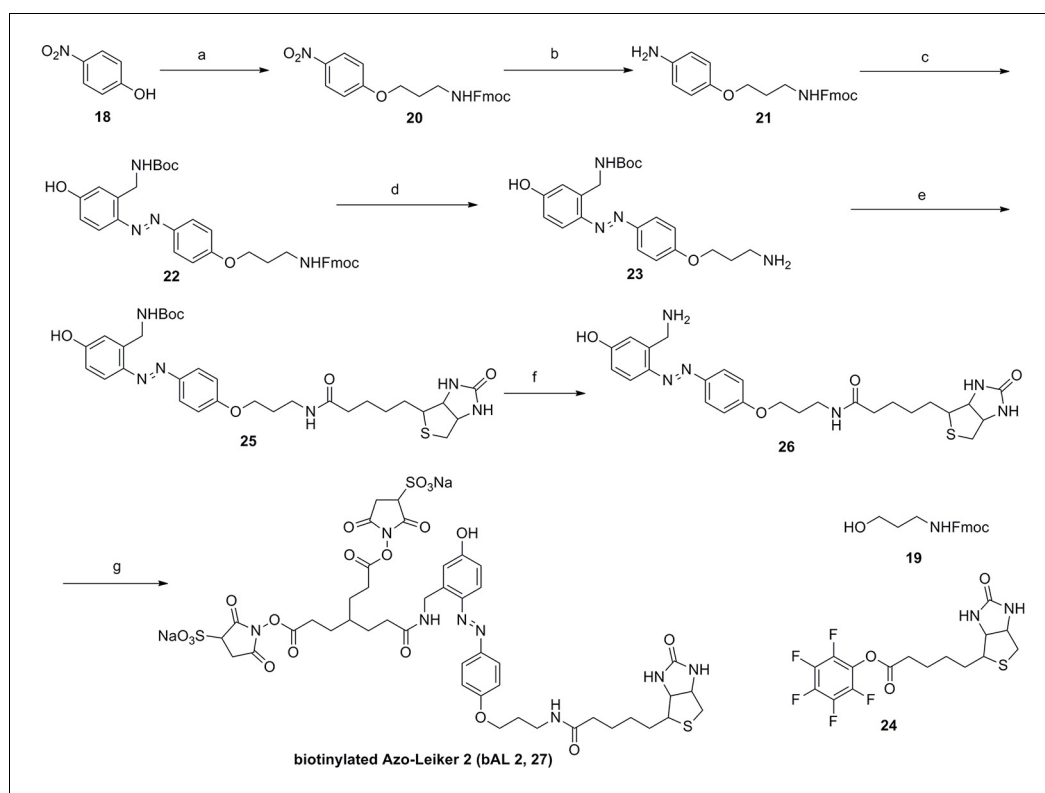
Appendix 1—figure 12. Compound 16.

DOI: [10.7554/eLife.12509.051](https://doi.org/10.7554/eLife.12509.051)



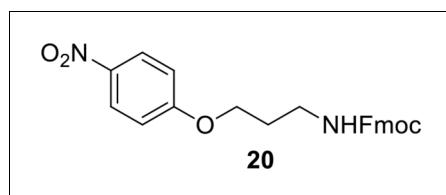
Appendix 1—figure 13. Compound 17.

DOI: [10.7554/eLife.12509.052](https://doi.org/10.7554/eLife.12509.052)



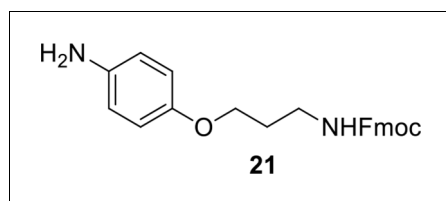
Appendix 1—figure 14. Synthesis of biotinylated Azo-Leiker 2 (bAL 2, 27).

DOI: [10.7554/eLife.12509.053](https://doi.org/10.7554/eLife.12509.053)



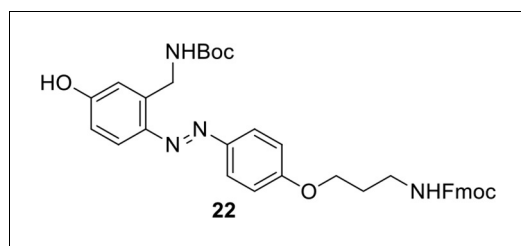
Appendix 1—figure 15. Compound 20.

DOI: [10.7554/eLife.12509.054](https://doi.org/10.7554/eLife.12509.054)



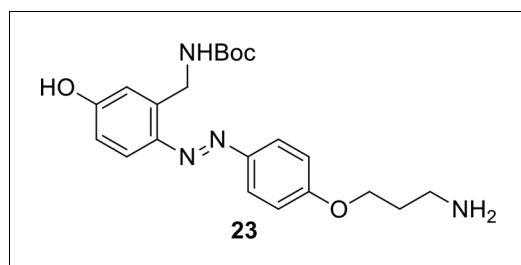
Appendix 1—figure 16. Compound 21.

DOI: [10.7554/eLife.12509.055](https://doi.org/10.7554/eLife.12509.055)



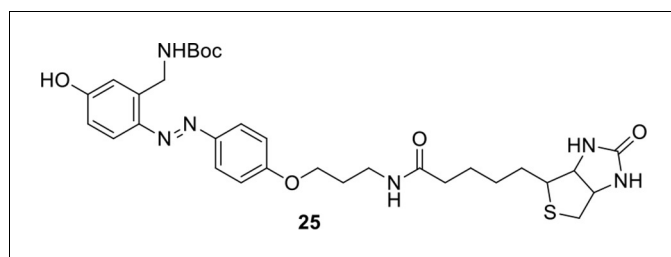
Appendix 1—figure 17. Compound 22.

DOI: [10.7554/eLife.12509.056](https://doi.org/10.7554/eLife.12509.056)



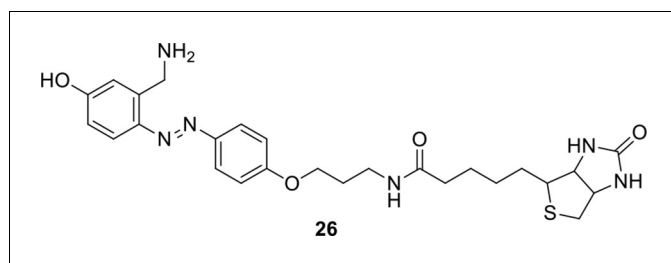
Appendix 1—figure 18. Compound 23.

DOI: [10.7554/eLife.12509.057](https://doi.org/10.7554/eLife.12509.057)



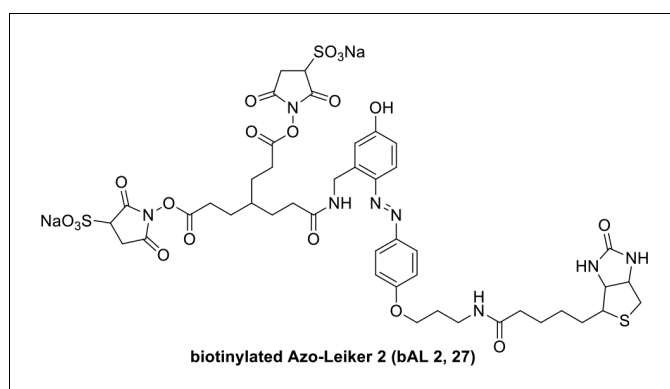
Appendix 1—figure 19. Compound 25.

DOI: 10.7554/eLife.12509.058



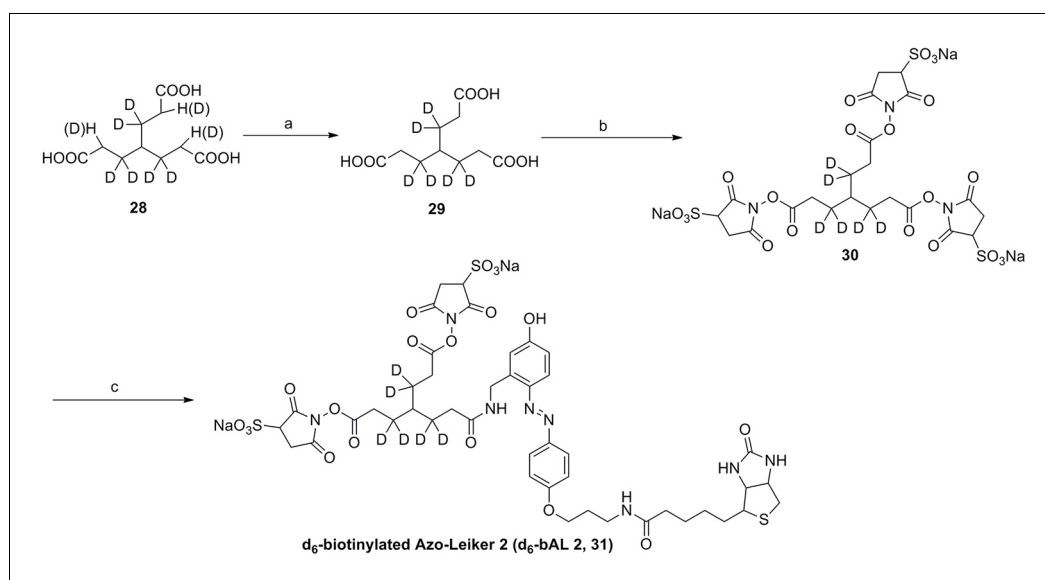
Appendix 1—figure 20. Compound 26.

DOI: [10.7554/eLife.12509.059](https://doi.org/10.7554/eLife.12509.059)



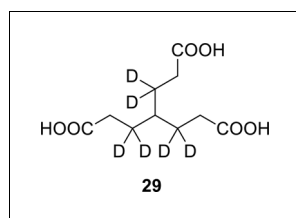
Appendix 1—figure 21. Compound 27.

DOI: [10.7554/eLife.12509.060](https://doi.org/10.7554/eLife.12509.060)



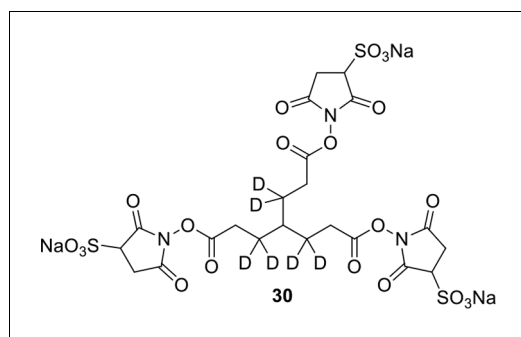
Appendix 1—figure 22. Synthesis of d_6 -biotinylated Azo-Leiker 2 (bAL 2, 31).

DOI: [10.7554/eLife.12509.061](https://doi.org/10.7554/eLife.12509.061)



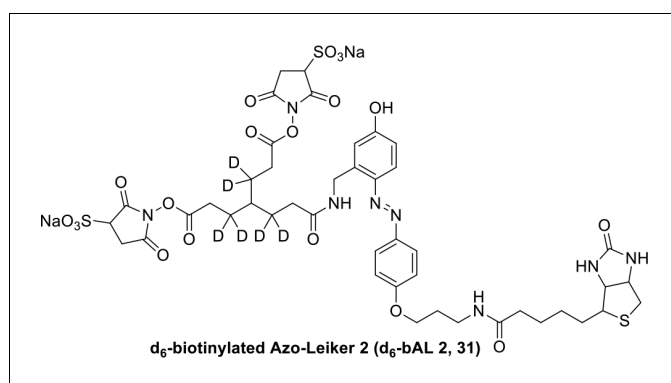
Appendix 1—figure 23. Compound 29.

DOI: [10.7554/eLife.12509.062](https://doi.org/10.7554/eLife.12509.062)



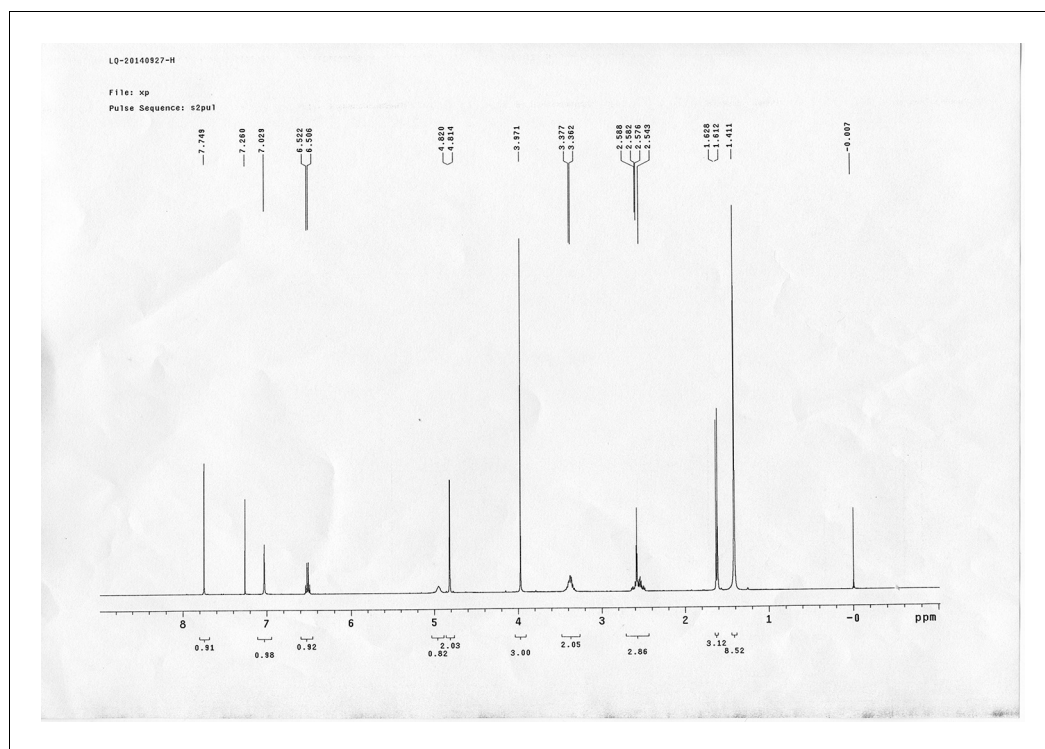
Appendix 1—figure 24. Compound 30.

DOI: [10.7554/eLife.12509.063](https://doi.org/10.7554/eLife.12509.063)



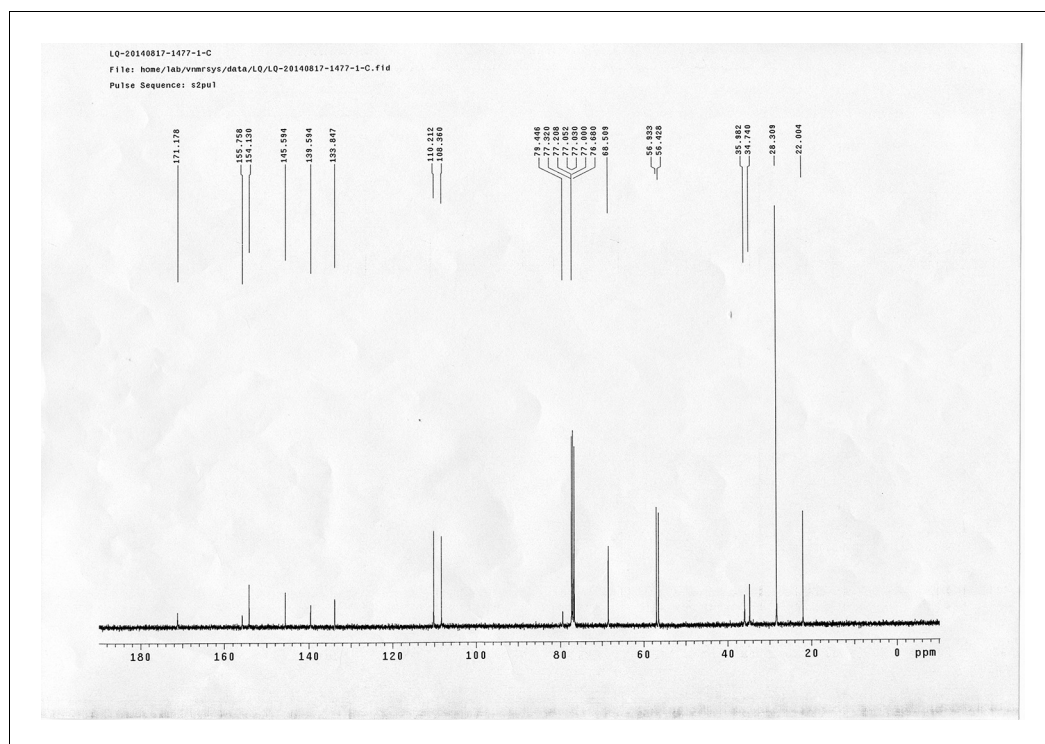
Appendix 1—figure 25. Compound 31.

DOI: [10.7554/eLife.12509.064](https://doi.org/10.7554/eLife.12509.064)



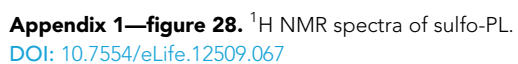
Appendix 1—figure 26. ^1H NMR spectra of compound 6.

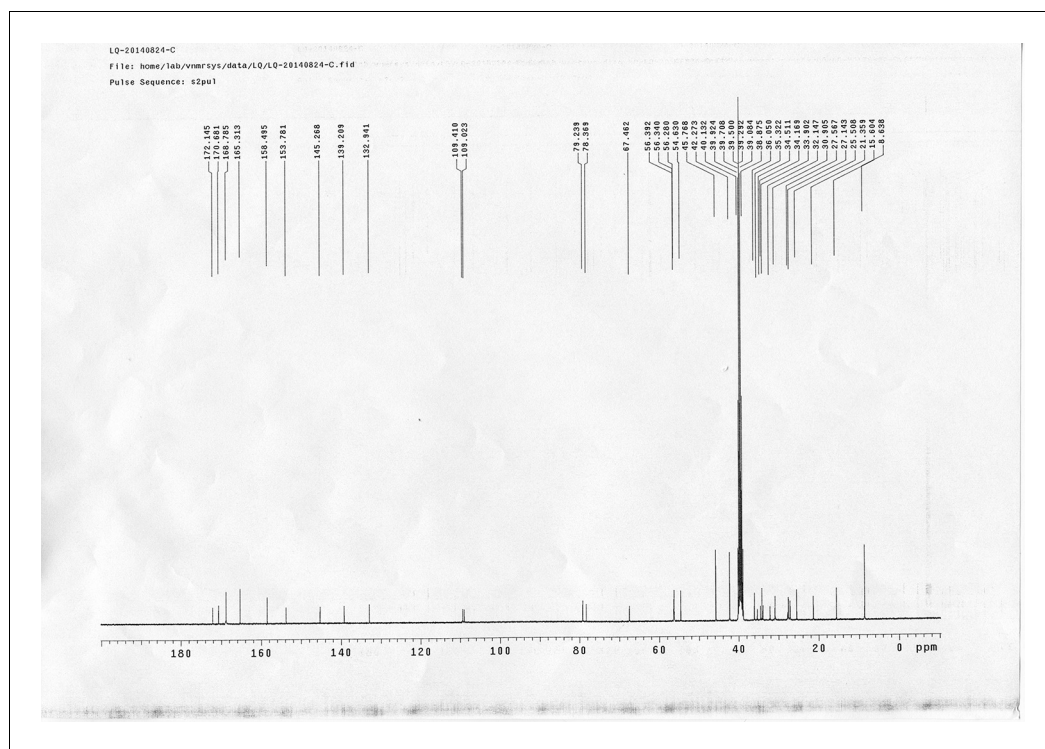
DOI: [10.7554/eLife.12509.065](https://doi.org/10.7554/eLife.12509.065)



Appendix 1—figure 27. ^{13}C NMR spectra of compound 6.

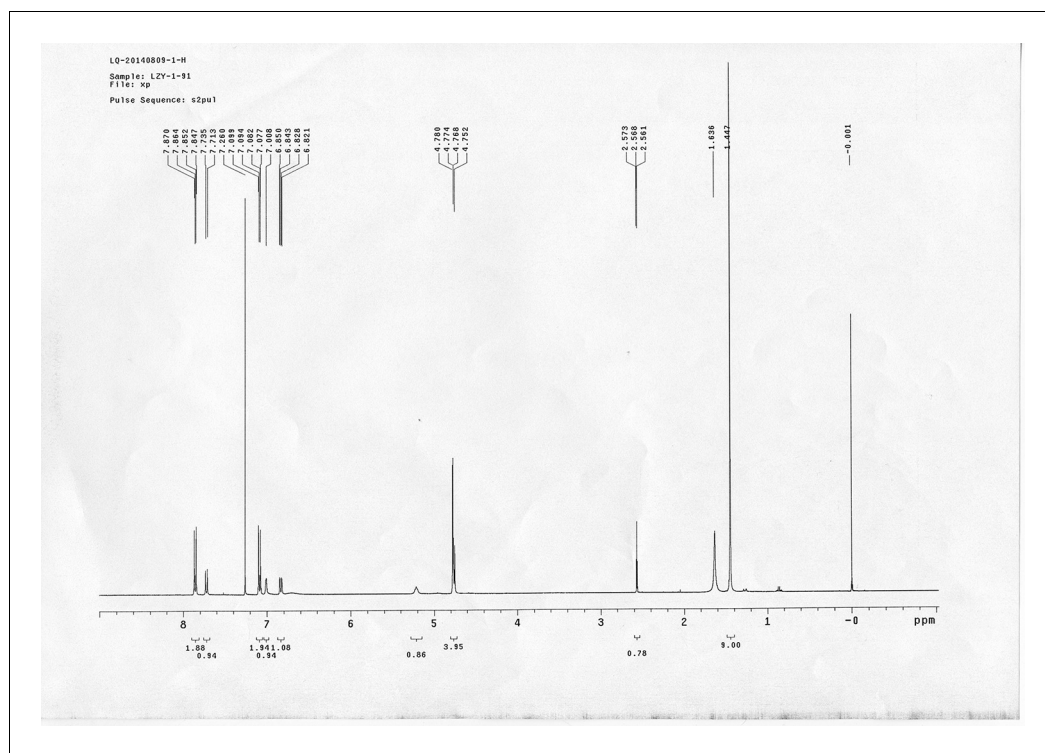
DOI: [10.7554/eLife.12509.066](https://doi.org/10.7554/eLife.12509.066)





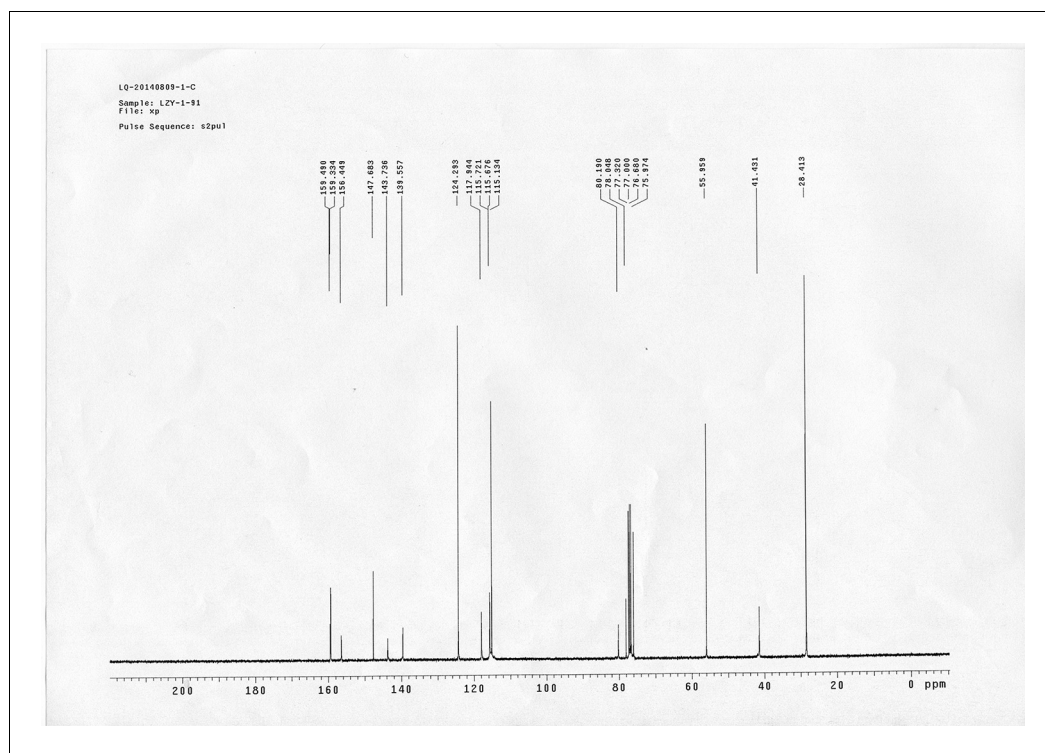
Appendix 1—figure 29. ^{13}C NMR spectra of sulfo-PL.

DOI: [10.7554/eLife.12509.068](https://doi.org/10.7554/eLife.12509.068)



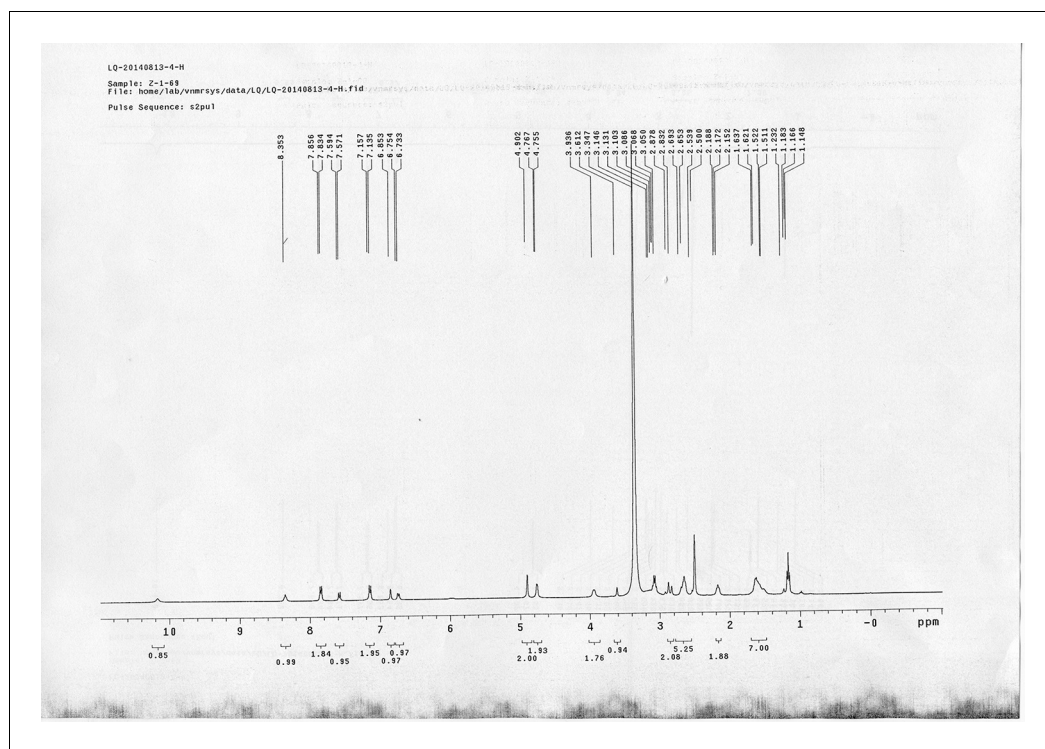
Appendix 1—figure 30. ^1H NMR spectra of compound 11.

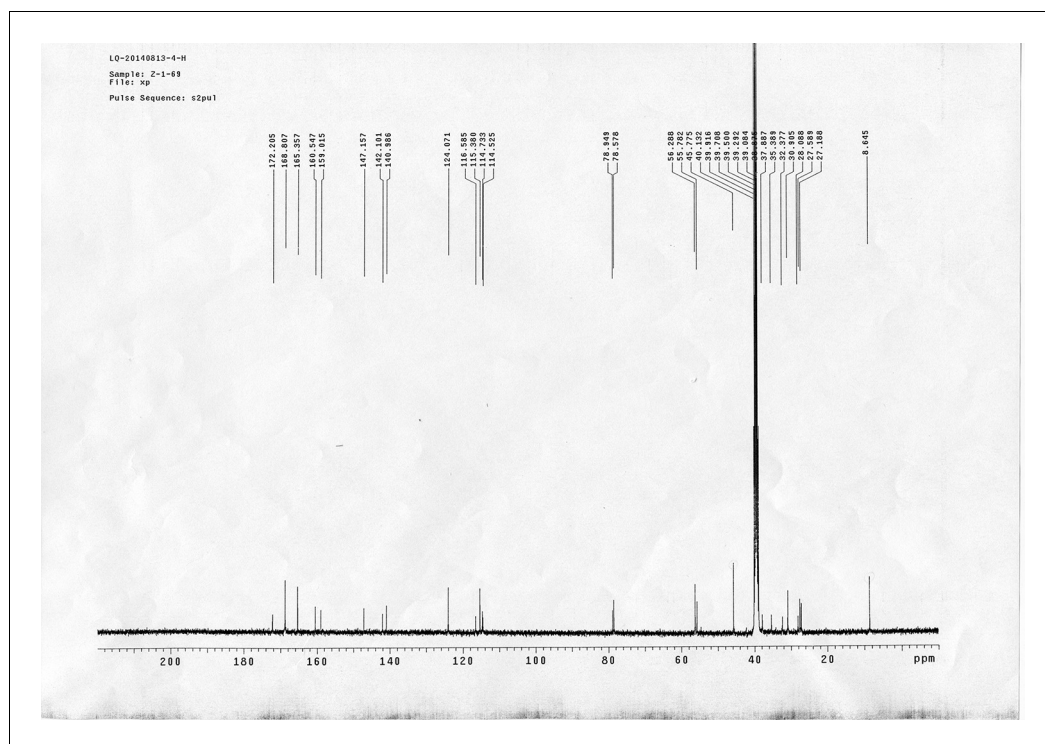
DOI: [10.7554/eLife.12509.069](https://doi.org/10.7554/eLife.12509.069)



Appendix 1—figure 31. ^{13}C NMR spectra of compound 11.

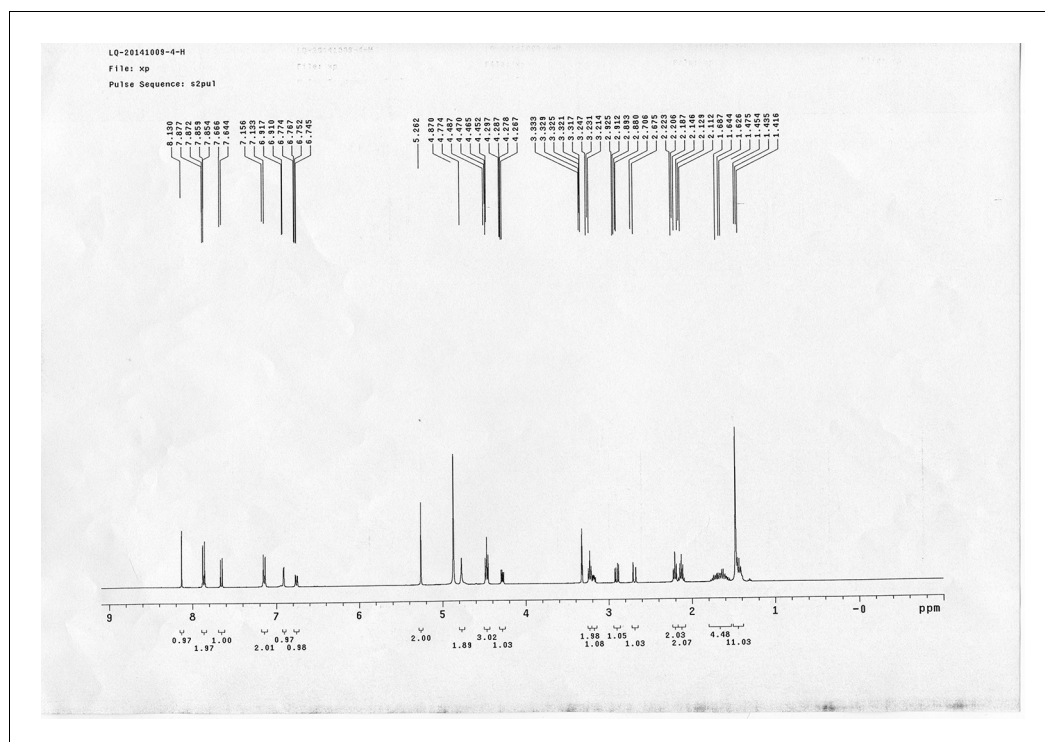
DOI: [10.7554/eLife.12509.070](https://doi.org/10.7554/eLife.12509.070)





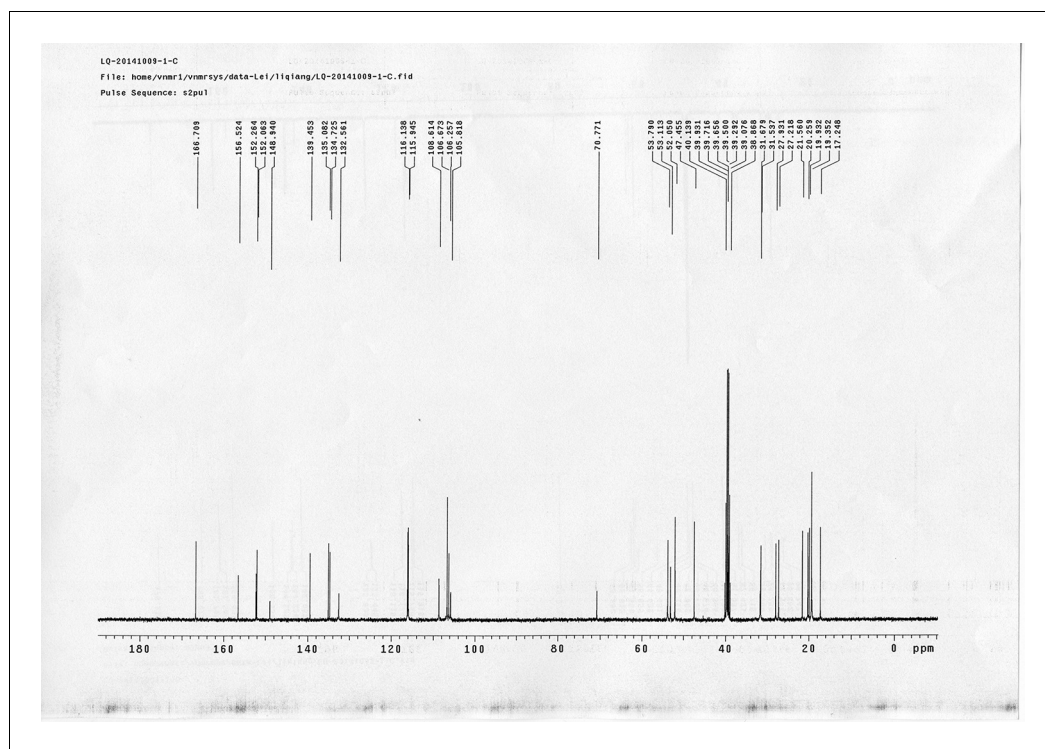
Appendix 1—figure 33. ^{13}C NMR spectra of AL.

DOI: [10.7554/eLife.12509.072](https://doi.org/10.7554/eLife.12509.072)



Appendix 1—figure 34. ^1H NMR spectra of compound 15.

DOI: [10.7554/eLife.12509.073](https://doi.org/10.7554/eLife.12509.073)

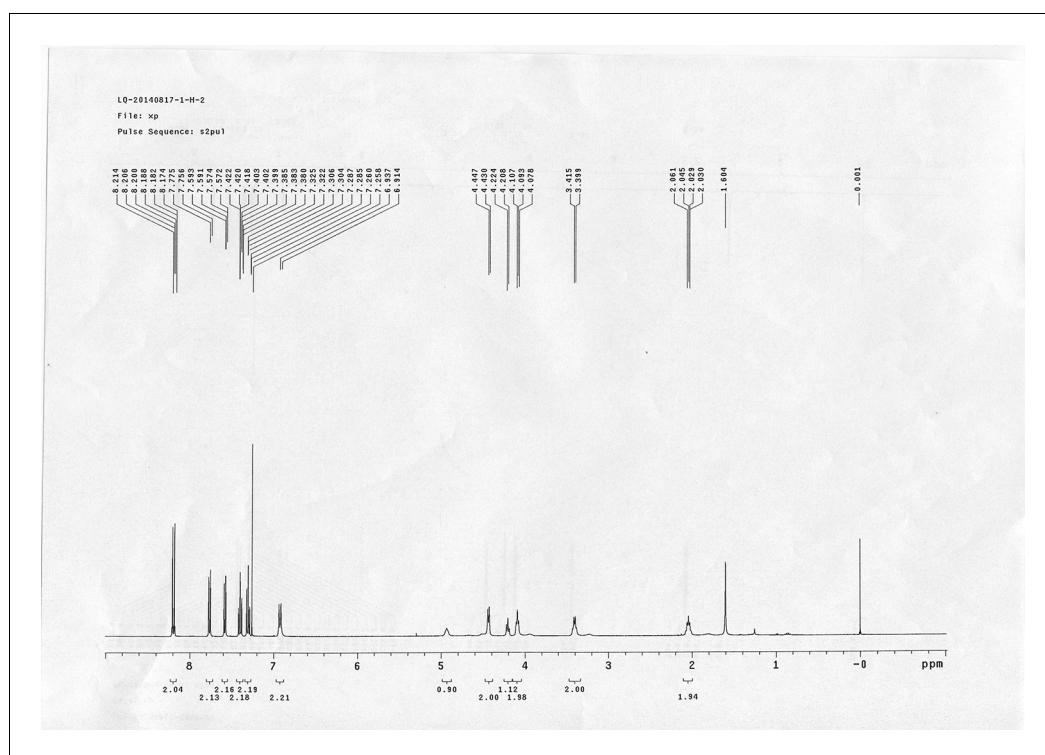


Appendix 1—figure 35. ^{13}C NMR spectra of compound 15.

DOI: [10.7554/eLife.12509.074](https://doi.org/10.7554/eLife.12509.074)

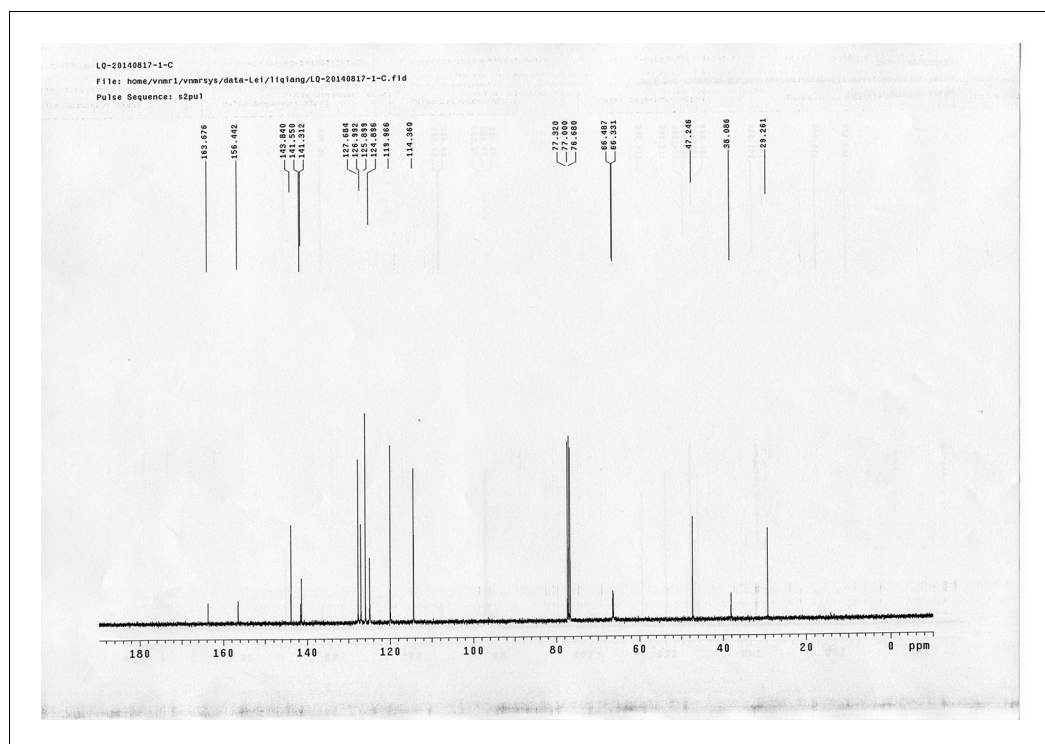






Appendix 1—figure 38. ^1H NMR spectra of compound 20.

DOI: [10.7554/eLife.12509.077](https://doi.org/10.7554/eLife.12509.077)

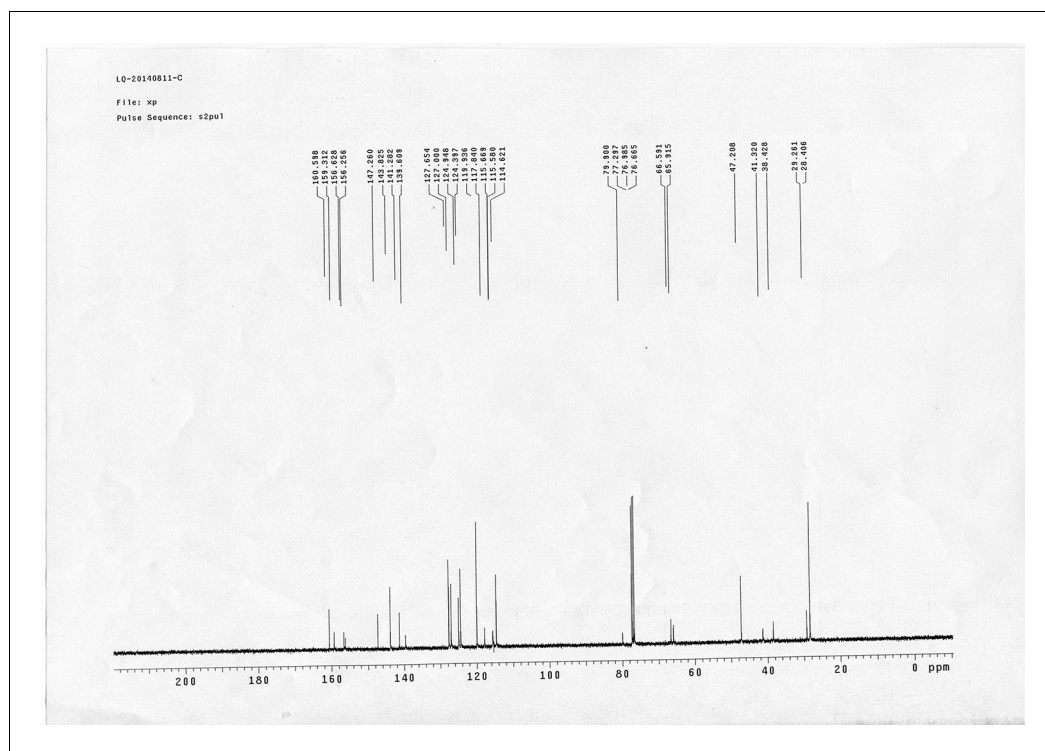


Appendix 1—figure 39. ^{13}C NMR spectra of compound 20.

DOI: [10.7554/eLife.12509.078](https://doi.org/10.7554/eLife.12509.078)

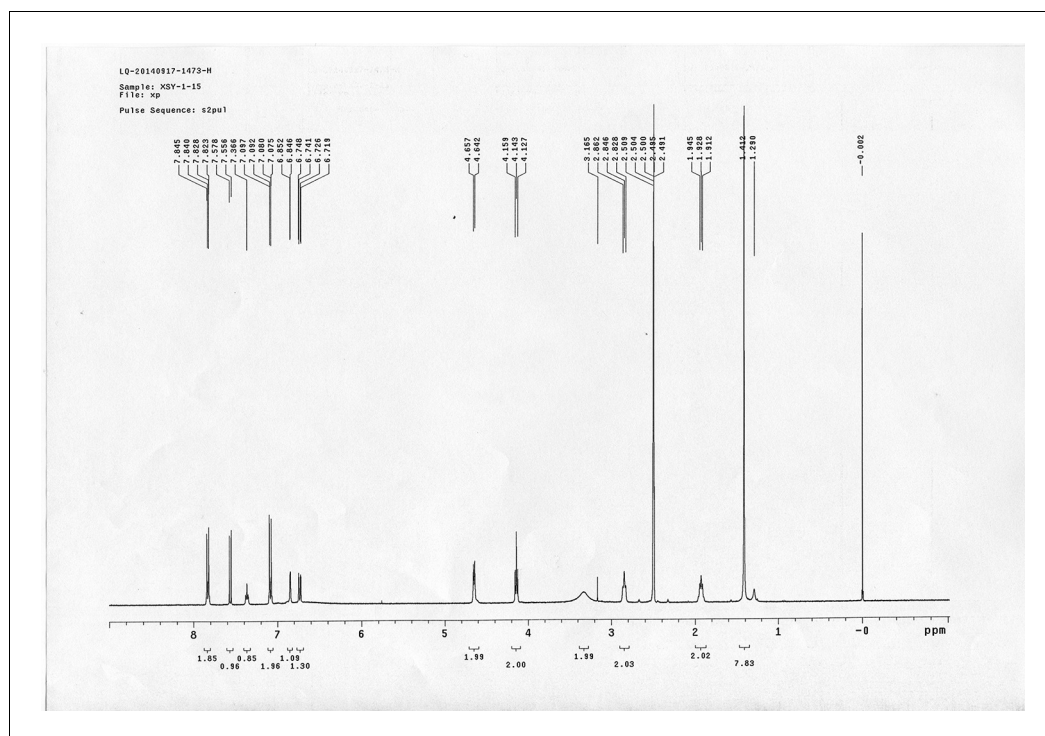


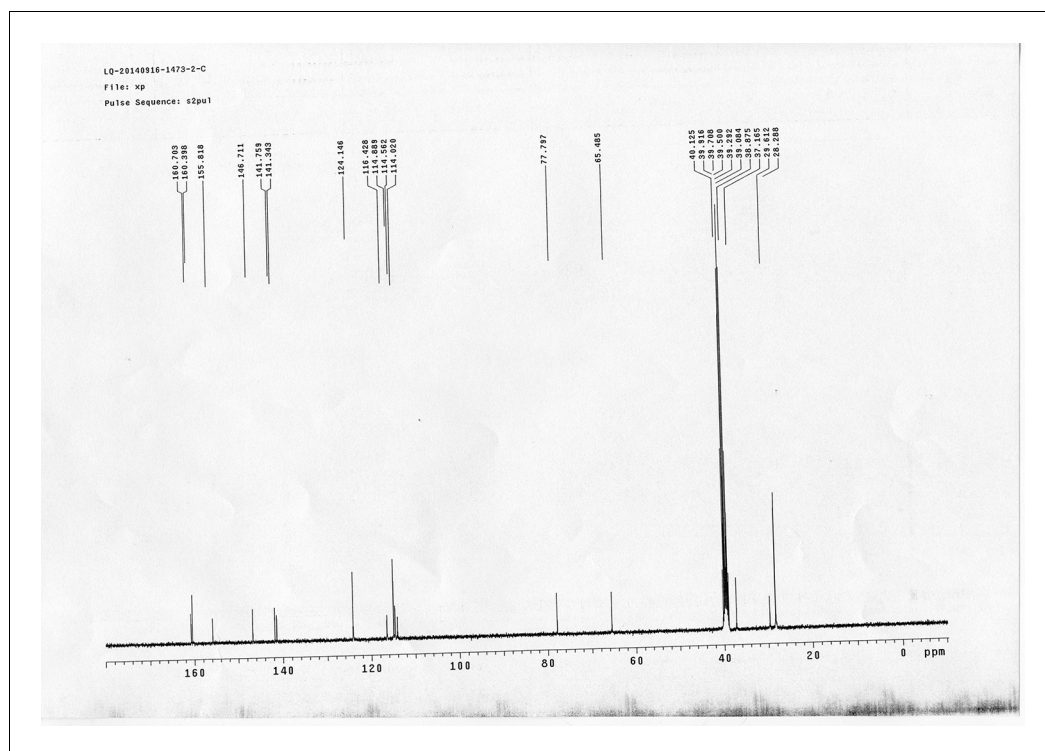




Appendix 1—figure 43. ^{13}C NMR spectra of compound 22.

DOI: [10.7554/eLife.12509.082](https://doi.org/10.7554/eLife.12509.082)

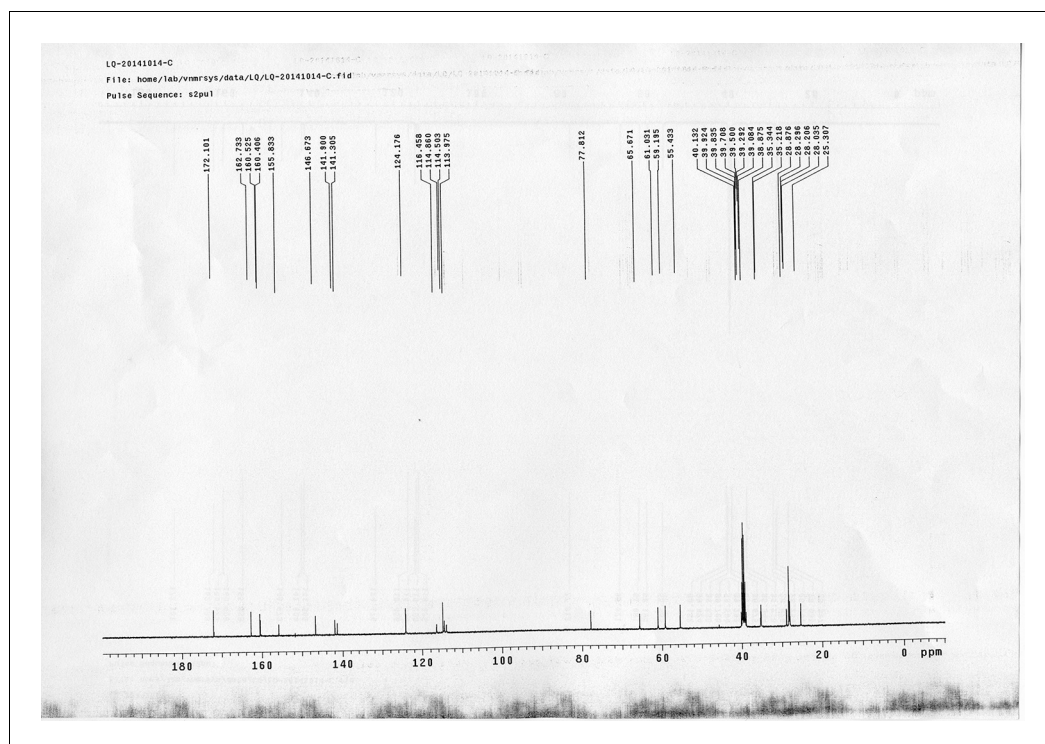




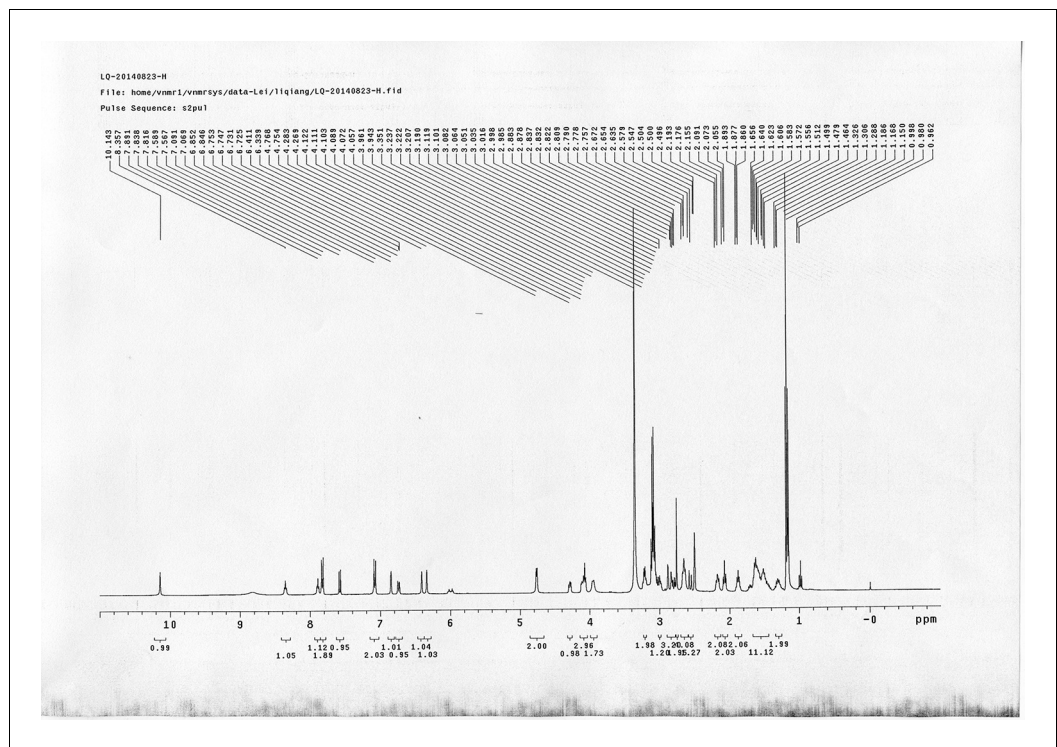
Appendix 1—figure 45. ^{13}C NMR spectra of compound 23.

DOI: [10.7554/eLife.12509.084](https://doi.org/10.7554/eLife.12509.084)





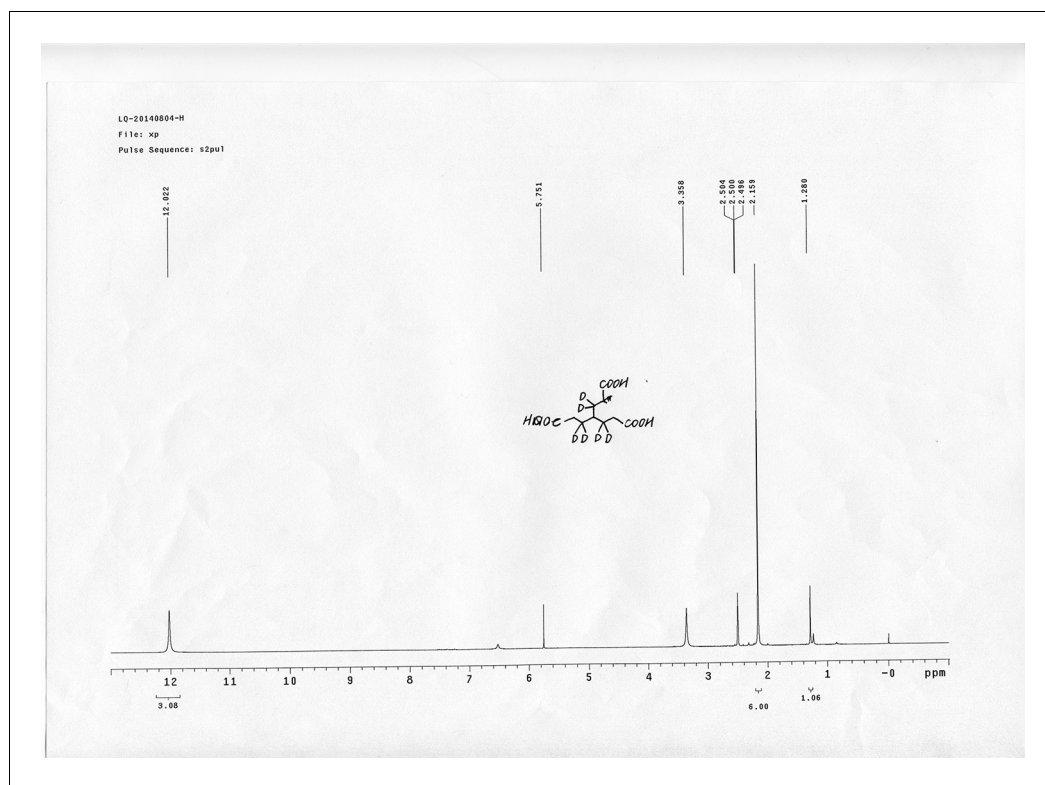
Appendix 1—figure 47. ^{13}C NMR spectra of compound 25.
DOI: [10.7554/eLife.12509.086](https://doi.org/10.7554/eLife.12509.086)



Appendix 1—figure 48. ^1H NMR spectra of bAL 2.

DOI: [10.7554/eLife.12509.087](https://doi.org/10.7554/eLife.12509.087)

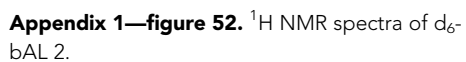




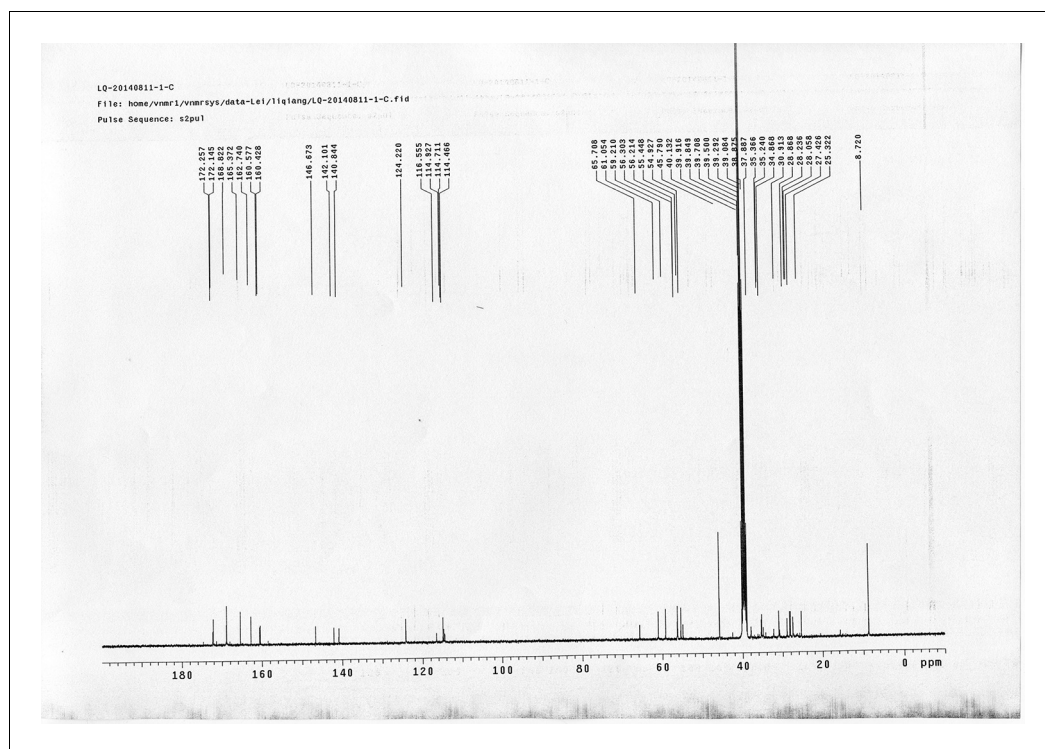
Appendix 1—figure 50. ^1H NMR spectra of compound 29.

DOI: [10.7554/eLife.12509.089](https://doi.org/10.7554/eLife.12509.089)





Tan et al. eLife 2016;5:e12509. DOI: [10.7554/eLife.12509](https://doi.org/10.7554/eLife.12509)



Appendix 1—figure 53. ^{13}C NMR spectra of d₆-bAL 2.

DOI: [10.7554/eLife.12509.092](https://doi.org/10.7554/eLife.12509.092)